Advanced Target Tracking Techniques

Wolfgang Koch

FGAN-FKIE
Neuenahrer Strasse 20
D 53343 Wachtberg, Germany
Tel +49 228 9435 373
Fax +49 228 9435 685

email w.koch@fgan.de

Abstract

In many engineering applications, including surveillance, guidance, or navigation, single stand-alone sensors or sensor networks are used for collecting information on time varying quantities of interest, such as kinematical characteristics and measured attributes of moving or stationary objects of interest (e.g. maneuvering air targets, ground moving vehicles, or stationary movers such as a rotating antennas).

More strictly speaking, in these applications the state vectors of stochastically moving objects are to be estimated from a series of sensor data sets, also called scans or data frames. The individual measurements are produced by the sensors at discrete instants of time, being referred to as scan or frame time, target revisit time, or data innovation time. These output data (sensor reports, observations, returns, hits, plots) typically result from complex estimation procedures themselves characterizing particular waveform parameters of the received sensor signals (signal processing).

In case of moving point-source objects or small extended objects, i.e. typical radar targets, often relatively simple statistical models can be derived from basic physical laws describing their temporal behavior and thus defining the underlying dynamical system. In addition, appropriate sensor models are available or can be constructed, which characterize the statistical properties of the produced sensor data sufficiently correct.

*As an introduction to **advanced target tracking techniques** characteristic problems occurring in typical radar applications are presented; key ideas relevant for their solution are discussed.*

Contents

1   Discussion of the Basic Ideas

In many engineering applications, including surveillance, guidance, or navigation, single stand-alone sensors or sensor networks are used for collecting information on time varying quantities of interest, such as kinematical characteristics and measured attributes of moving or stationary objects of interest (e.g. maneuvering air targets, ground moving vehicles, or stationary movers such as a rotating antennas).

More strictly speaking, in these applications the state vectors of stochastically moving objects are to be estimated from a series of sensor data sets, also called scans or data frames. The individual measurements are produced by the sensors at discrete instants of time, being referred to as scan or frame time, target revisit time, or data innovation time. These output data (sensor reports, observations, returns, hits, plots) typically result from complex estimation procedures themselves characterizing particular waveform parameters of the received sensor signals (signal processing).

In case of moving point-source objects or small extended objects, i.e. typical radar targets, often relatively simple statistical models can be derived from basic physical laws describing their temporal behavior and thus defining the underlying dynamical system. In addition, appropriate sensor models are available or can be constructed, which characterize the statistical properties of the produced sensor data sufficiently correct.

As an introduction to advanced target tracking techniques characteristic problems occurring in typical radar applications are presented; key ideas relevant for their solution are discussed.

1.1   Sensor Data Exploitation: Tracking

Let us assume a single stand-alone radar sensor or a sensor network (distributed or co-located) producing measurements which characterize the kinematical parameters of certain objects of interest such as range, azimuth, or radial velocity with respect to the sensors' position. In addition, certain types of sensors can be considered delivering attribute type measurements, which provide information of the objects' characteristic properties and thus can be used for target classification or even identification.

For efficiently exploiting the sensor resources available as well as for gaining information not directly given by the individual sensor reports themselves, appropriate sensor data exploitation algorithms are required. These techniques for a "post-production processing" of the sensor data basically consist in a temporal integration and a logical analysis of the data by exploiting statistical estimation and data association methods. In this context also the combination of the data with available background information ("context knowledge") is an important aspect. These sensor data processing techniques result in tracks, i.e. estimates of state trajectories, which statistically represent the currently available knowledge of an object of interest along with its temporal history. Important parts of the tracks are characteristic quality measures, which quantitatively describe the reliability or precision of this information.

In the two lectues devoted to target tracking and data fusion aspects we address characteristic target tracking tasks and sketch the structure and potential use of more advanced algorithms being relevant for designing tracking systems. By selected examples their potential in view of real radar applications are demonstrated. The results can directly be transfered to stand-alone sensors and measurement fusion, but are also the basic elements for designing more sophisticated sensor data fusion architectures.

1.2   Characteristic Problem: Ambiguity

In many practical applications the tracking problem is characterized by uncertainty and ambiguities, which are inherent constituents of the underlying scenario and the sensor systems used for observing targets in a region of interest. The BAYESian approach being discussed in the subsequent sections is a well-suited methodology for dealing with those phenomena. More abstractly speaking, BAYESian tracking is essentially a processing scheme for dealing with uncertain information (of a particular type), which allows to make "soft" or "delayed" decisions as long as it is not possible to form a unique decision according to the particular data situation currently to be dealt with.

Ambiguities can have many different causes: The sensors may produce ambiguous data due to their limited resolution capabilities or phenomena such a Doppler blindness in MTI radar applications (MTI: Moving Target Indicator). Often an additional source of ambiguities is the environment of the object to be tracked itself. There can well exist dense object situations, residual clutter nor being suppressed of the radar's clutter filter, man-made noise, or simply unwanted targets (e.g. birds). A more indirect type of ambiguities can raise from the properties of the object to be tracked, for example if it shows qualitatively distinct maneuvering phases. Finally, the potential background knowledge to be used may imply problem-inherent ambiguities such as road maps with their intersections or tactical rules describing the over-all behavior of the objects to be tracked.

1.3   Multiple Objects: Sensor Resolution

Due to the limited resolution capabilities of every physical sensor, closely-spaced objects moving as a group for a time will continuously transition from being resolved to unresolved and back again.

As an example let us consider a medium range radar producing range and azimuth measurements for a target formation consisting of two targets. In case of a resolution conflict an unresolved radar plot can be interpreted as a measurement of the group center. For physical reasons the resolution in range, azimuth, and range-rate will be independent from each other. In particular, range and cross-range resolution differ significancy in many radar applications. Therefore the resolution performance of the sensor is expected to depend strongly on the current sensor-to-group geometry and the relative orientation of the targets within the group. The sensor's resolution capability also determined by the particular signal processing techniques used and the random target fluctuations. As a complete description is rather complicated, we have to look for a simplified, but qualitatively correct and mathematically tractable model.

In any case, the radar resolution capability in range and azimuth is limited by the corresponding band- and beam-width. These radar specific parameters must explicitly enter into any processing of possibly unresolved plots. The typical size of resolution cells in a medium distance is about 50 m (range) and 500 m (cross range). As in target formations the mutual distance may well be 50 - 500 m or even less, the limited sensor resolution is a real problem in target tracking [6]. Evidently, resolution phenomena will be observed if the range and angular distances between the targets are small compared with the resolution parameters. On the other hand, the targets within the group are resolvable if the opposite is true. Furthermore we expect a narrow transient region. A more quantitative description is provided by introducing a probability of being unresolved P_u depending on the sensor-to-group geometry. For this quantity in subsection 3.2.3 a simple model is discussed.

As an example let us consider the simplified situation in Figure 1a. A formation with two targets is passing a radar. We here consider an echelon formation. R is the minimum distance of the group center from the radar. Figure 1b shows the resulting probability $P_u(r; R)$ parameterized by $R = 0, 10, 30, 60$ km as a function of the distance r between the formation center and the radar. The solid lines refer to a formation approaching the radar ($\dot{r} < 0$), the dashed lines refer to $\dot{r} > 0$. For $R \neq 0$ both flight phases differ substantially. Near R the probability P_u varies strongly ($0.85 \rightarrow 0.15$). For a radial flight ($R = 0$) we observe no asymmetry and P_u is constant over a wide range ($r \gg r_c$). This discussion makes evident, that radar resolution capability strongly depends on the underlying sensor-to-target geometry and the relative position of the targets within the group.

1.4   Description by Probability Densities

Many basic ideas and mathematical techniques relevant to the design of tracking systems can be discussed in a unified statistical framework that essentially makes use of BAYES' Rule. The general multiple-object, multiple-sensor tracking task, however, is highly complex and involves rather sophisticated combinatorial and logical considerations that are beyond the scope of this tutorial. For a more detailed discussion of the

a. scenario   b. resolution
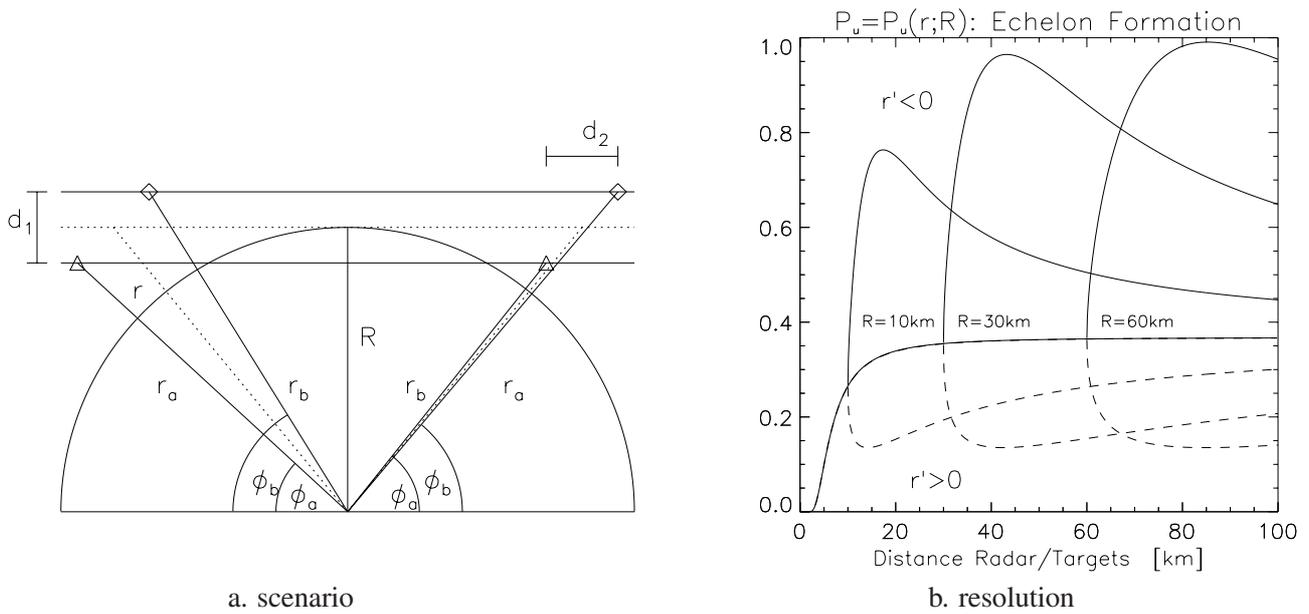
Figure 1: Resolution (Effect of Sensor-to-Target Geometry)

problems involved see [4] and the literature cited therein. Nevertheless, in many applications the task can be partitioned into independent sub-problems of (much) less complexity.

In a BAYESian view, a tracking algorithm is an iterative updating scheme for conditional probability densities $p(\mathbf{x}_l | \mathcal{Z}^k)$. These densities represent all available knowledge on the kinematical state vectors $\mathbf{x}_l$ of the objects to be tracked at discrete instants of time t_l given both, the sensor data $\mathcal{Z}^k$ accumulated up to some time t_k, typically the current scan time, as well as all available a priori information (sensor characteristics, object dynamics, operating conditions, road and topographical maps, tactical rules, ...). Depending on the time t_l at which estimates for the state vectors $\mathbf{x}_l$ are required, the related estimation process is referred to as *prediction* ($t_l > t_k$), *filtering* ($t_l = t_k$), and *retrodiction* ($t_l < t_k$), respectively [9, 7, 17, 22]. Equation 1 illustrates schematically an iterative process for calculating the conditional probability densities $p(\mathbf{x}_l | \mathcal{Z}^k)$:

$$
\begin{array}{llll}
\text{prediction:} & p(\mathbf{x}_{k-1} | \mathcal{Z}^{k-1}) & \xrightarrow[\text{road/topographical maps}]{\text{dynamics model}} & p(\mathbf{x}_k | \mathcal{Z}^{k-1}) \\[2em]
\text{filtering:} & p(\mathbf{x}_k | \mathcal{Z}^{k-1}) & \xrightarrow[\text{sensor model}]{\text{current sensor data}} & p(\mathbf{x}_k | \mathcal{Z}^k) \\[2em]
\text{retrodiction:} & p(\mathbf{x}_{l-1} | \mathcal{Z}^k) & \xleftarrow[\text{dynamics model}]{\text{filtering output}} & p(\mathbf{x}_l | \mathcal{Z}^k).
\end{array}
\tag{1}
$$

Under the conditions previously discussed, the densities have a particular formal structure: They are finite mixtures, i.e. weighted sums of individual densities that assume particular data interpretations and model hypotheses to be true. This structure is thus a direct consequence of the uncertain origin of the sensor data and of the uncertainty related to the underlying system dynamics. Provided the densities $p(\mathbf{x}_l | \mathcal{Z}^k)$ are calculated correctly, optimal estimators may be derived related for various risk functions adapted to the applications.

Evidently, iteratively defined tracking algorithms must be initiated by appropriately chosen a priori densities (track initiation, track extraction [12, 11]). This is a relatively simple task provided the sensor reports are actually valid measurements of the objects to be tracked. For low observable objects, i.e. targets embedded in a high false return background, however, more than a single frame of observations are unusually

(a) forward iteration   (b) backward iteration
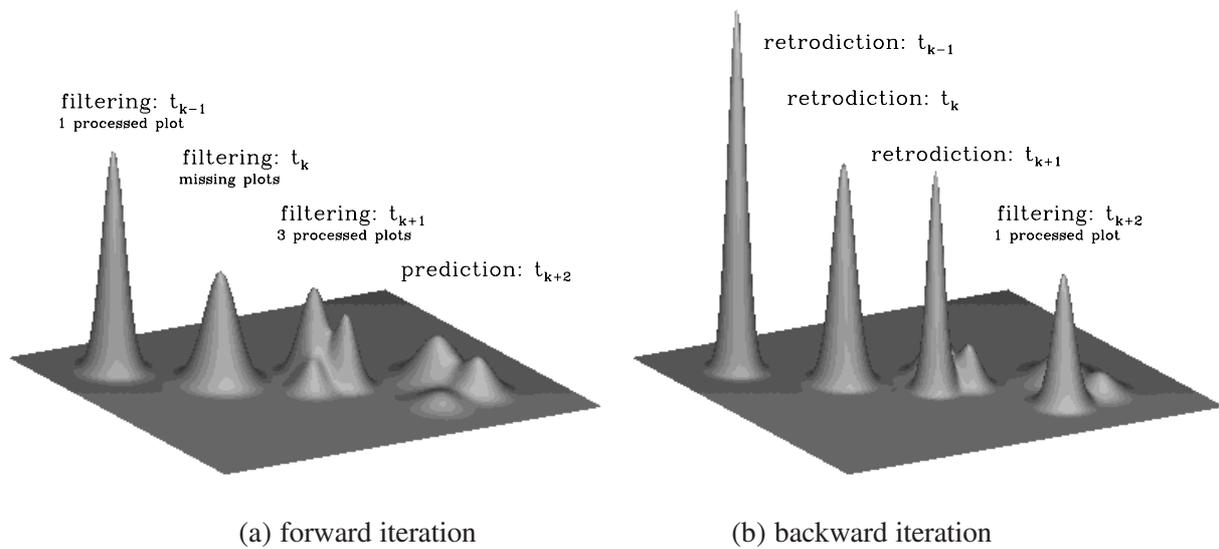
Figure 2: Scheme of BAYESian Density Iteration

necessary for detecting all objects of interest moving in the sensors' field of view. By this, a higher level detection process is defined resulting in algorithms for multiple-frame track extraction (see subsection 3.6).

Figure 2 provides a schematic illustration of the BAYESian density iteration scheme. The probability densities $p(\mathbf{x}_{k-1}|\mathcal{Z}^{k-1})$, $p(\mathbf{x}_k|\mathcal{Z}^k)$, and $p(\mathbf{x}_{k+1}|\mathcal{Z}^{k+1})$ resulting from filtering at the scan times t_{k-1}, t_k, and t_{k+1}, respectively, are displayed along with the predicted density $p(\mathbf{x}_{k+2}|\mathcal{Z}^{k+1})$ (Figure 2a, forward iteration). While at time t_{k-1} one sensor report has been processed, no report could be associated to the track at time t_k. Hence a missing detection according to a detection probability < 1 is assumed. As a consequence of this lack of sensor information, the density $p(\mathbf{x}_k|\mathcal{Z}^k)$ is broadened, because target maneuvers may have occurred. This in particular implies an increased correlation gate for the subsequent scan time t_{k+1}. According to this effect, at time t_{k+1} three correlating sensor reports are to be processed leading to a multi-modal probability density. The multiple modes reflect the ambiguity regarding the origin of the sensor data and characterize also the predicted density $p(\mathbf{x}_{k+2}|\mathcal{Z}^{k+1})$. By this, the data-driven adaptivity of the BAYESian updating scheme is clearly indicated. In Figure 2b the density $p(\mathbf{x}_{k+2}|\mathcal{Z}^{k+2})$ resulting from processing a single correlating report at t_{t+2} along with the retrodicted densities $p(\mathbf{x}_{k+1}|\mathcal{Z}^{k+2})$, $p(\mathbf{x}_k|\mathcal{Z}^{k+2})$, and $p(\mathbf{x}_{k-1}|\mathcal{Z}^{k+2})$ are shown. Evidently, newly available sensor data significantly improve the estimates of the past states.

1.5 Discussion of an Example: Dog-fights

Track initiation and maintenance by processing noise corrupted sensor returns is by no means a trivial task if the sensor data are of uncertain origin or if there exists uncertainty regarding the underlying system dynamics. With an example with real radar data recorded during a dog-fight exercise we mainly focus on four aspects:

1. Data association conflicts arise even for well-separated objects if a high false return background is to be taken into account, which was not completely suppressed by clutter filtering.

2. Even in the absence of unwanted sensor reports, ambiguous correlations between newly received sensor reports and existing tracks are an inherent problem for objects moving closely-spaced for some time.

3. Additional problems arise from sensor returns having a poor quality, due to large measurement errors, low signal-to-noise ratios, or fading phenomena (i.e. successively missing plots), for instance.

4. Besides that, the scan rates may be low in certain applications, such as long-range air surveillance. Furthermore, resolution phenomena make the data association problem task even harder.

5. In a given mission often clearly distinct maneuvering phases can be identified, as even agile targets do not always use their high maneuvering capability. Nevertheless, sudden switches between the underlying dynamics models do occur and are to be taken into account.

Figure 3a shows a radar data set accumulated over about 50 min. Besides many false alarms (probably due to ground clutter) the data of two pairs of interceptor aircraft performing an air combat exercise were recorded.

The detection probability is fairly low (40–60%). In addition rather long sequences of missed detections occur (fading phenomena). The clutter density is about .002 /km^2. The data were collected from a rotating S-band long-range radar. Range and azimuth information was used only; the elevation data were corrupted and thus ignored. The radar is characterized by the following parameters: scan period: 10 sec, range accuracy: 350 ft, bearing accuracy: .22°, range resolution: 1600 ft, bearing resolution: 2.4°.

Information on the real target position is crucial for evaluating tracking filters. This is particularly true under conditions where even trained human observers seem unable to assess the filtering output. Here a secondary radar was used: When primary and secondary radar produced identical information (within a certain correlation gate), the primary plots received an ID number. The target ID served for track assessment exclusively and was not used in the filtering algorithm. The verified primary plots are indicated by green and blue dots in Figure 3d,e along with the final tracking result obtained after processing the raw data (i.e. multiple hypothesis tracking (MHT) and and subsequent retrodiction).

Figure 3b shows the underlying hypothesis tree formed by the tracker in the first phase of dog-fight 1. The yellow dots indicate hypotheses related to target 1, while the orange dots refer to target 2. During the tracking process the number of targets involved (i.e. two) was assumed to be known. Right after the split-off maneuver the non-maneuvering target has to be tracked in presence of strong clutter interference and is thus likely to be lost if mono-hypothesis tracking algorithm were used. The leaves of the resulting hypothesis tree in Figure 3b represent the knowledge of the targets' kinematical state at the present time. The impact of retrodiction on the available knowledge of the past target state is displayed in 3c. The blue dots indicate hypotheses, which could be deleted by exploiting sensor data which became available after the time when they were formed. The statistical weighting factors after their creation might well have been larger than the weight of the hypothesis produced by processing the true target measurement. Red and white are the trajectories finally found by applying retrodiction. Evidently, retrodiction does not improve the estimates at present. We can conclude that the ambiguities inherent in the sensor data can be removed by using retrodiction techniques at the expense of a certain time delay of some sensor scans. Even a delay of only two frames can significantly improve the filtering output.

1.6 Generic Scheme of a Tracking System

Figure 4 provides a schematic overview of a generic tracking system along with its relation to the underlying sensor system. In the subsequent sections its basic elements are being discussed in greater detail.

After passing the detector device, which essentially serves as a means of data rate reduction, the sensor signal processing unit provides estimates of signal parameters characterizing the waveforms received by the sensing hardware (e.g. radar antennas). From these preprocessed estimates sensor reports are formed, i.e. measured quantities possibly related to the objects of interest, that are input information for the tracking system. In the tracking system itself all sensor data, which can be associated to the already existing tracks, are used for track maintenance (prediction, filtering, retrodiction). The remaining non-associated data are processed in order to establish new tentative tracks (track initiation, multiple frame track extraction). The
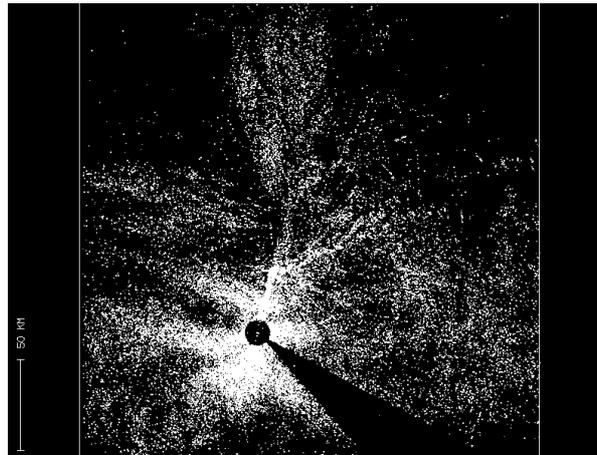
(a) accumulated radar data
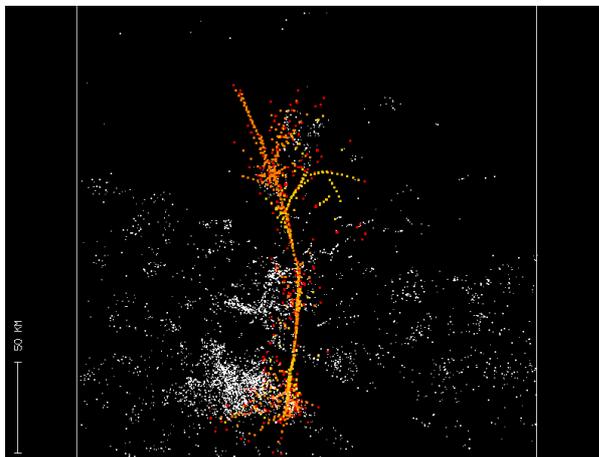
(b) MHT hypothesis tree
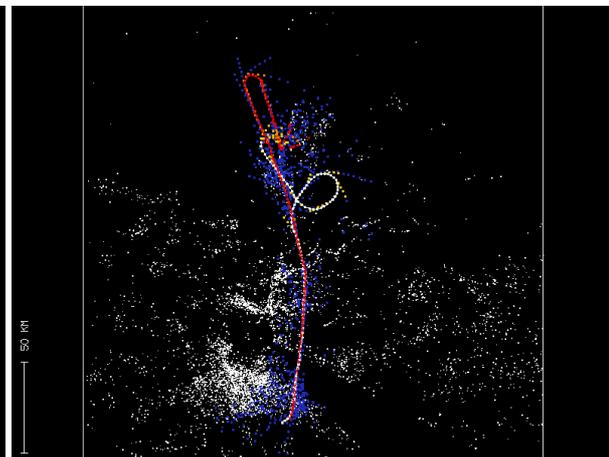
(c) retrodicted trajectory
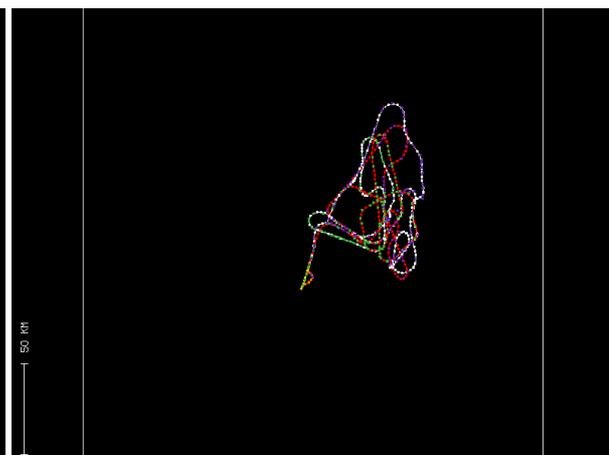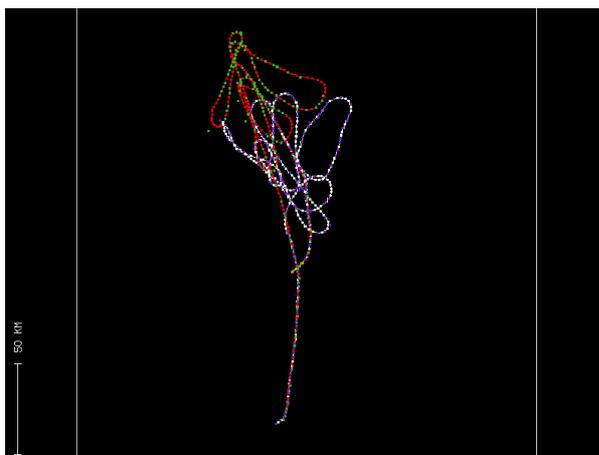
(d), (e) both dogfights with verified primary plots

Figure 3: A Typical Dog-fight Scenario

Tracking & Fusion System
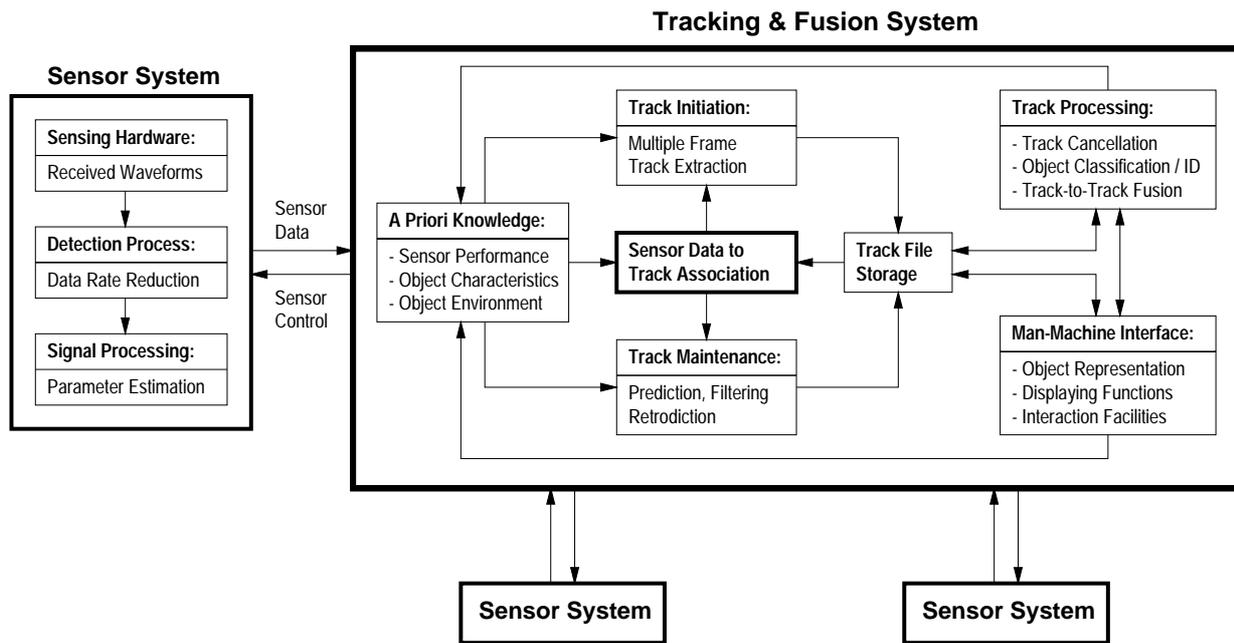
Figure 4: Generic Scheme of a Tracking System

plot-to-track association unit thus plays a key role in any multiple target tracking system. Evidently, a priori knowledge in terms of statistical models of the sensor performance, object characteristics (including their dynamical behavior), and the object environment is prerequisite to both track maintenance and track initiation. Track confirmation/termination, object classification/identification, and fusion of tracks representing identical information is performed in the track processing unit. The generic scheme of a tracking system is completed by a man-machine interface with displaying and interaction functions. The available information on the sensor, the objects of interest, and the environment can be specified, updated, or corrected by direct human interaction as well as by the track processor itself, e.g. as a consequence of a successful object classification.

2   BAYESian Approach to Target Tracking

Following the spirit of the preliminary discussion in the introduction we briefly summarize along which lines how we shall proceed:

- **Basis:** In the course of time one or several sensors produce 'measurements' of one or several targets of interest. The accumulated sensor data an example of a 'time series'. Each targets is characterized by its current 'state', a vector typically consisting of the current target position, its velocity, and acceleration. The target state is expected to change with time.

- **Objective:** Learn as much as possible about the individual target states at each time of interest by analyzing the 'time series' created by the sensor data.

- **Problem:** The sensor information is inaccurate, incomplete, and eventually even ambiguous. Moreover, the phenomena determining the targets' temporal evolution are usually not well-known.

- **Approach:** Interpret sensor measurements and target state vectors as random variables. Describe by the corresponding probability density functions (pdf) what is known about these random variables.

- **Solution:** Derive iteration formulae for calculating the probability density functions of the state variables and develop a mechanism for initiating the iteration. Derive state estimates from the densities along with appropriate quality measures.

2.1 Probability Densities: Selected Facts

Let us at first collect some facts from elementary probability theory to be used in the subsequent discussion:

1. Information of a random variable $\mathbf{x}$ is gained by *integrating* the corresponding probability density function $p(\mathbf{x})$. Integration over a volume V, i.e. $\int_V d\mathbf{x}\, p(\mathbf{x})$, yields the probability that the event '$\mathbf{x} \in V$' occurs. With this interpretation a pdf must be *non-negative*, $p(\mathbf{x}) \geq 0$, and *normalized*, $\int d\mathbf{x}\, p(\mathbf{x}) = 1$.

2. The *expectation* of $\mathbf{x}$ is defined by the integral $\mathbb{E}[\mathbf{x}] = \int d\mathbf{x}\, \mathbf{x}\, p(\mathbf{x})$, i.e. by the 'centroid' of its pdf. Another important expectation is the 'expected error of the expectation of $\mathbf{x}$', i.e. a quality measure for $\mathbb{E}[\mathbf{x}]$. It is defined by the integral (*covariance matrix*):

$$\mathbb{E}[(\mathbf{x} - \mathbb{E}[\mathbf{x}])(\mathbf{x} - \mathbb{E}[\mathbf{x}])^\top] = \int d\mathbf{x}\, (\mathbf{x} - \mathbb{E}[\mathbf{x}])(\mathbf{x} - \mathbb{E}[\mathbf{x}])^\top\, p(\mathbf{x}). \tag{2}$$

3. A *conditional probability density* $p(\mathbf{x}|\mathbf{y})$ of a random variable $\mathbf{x}$ describes how available knowledge about another random variable $\mathbf{y}$ affects our knowledge on $\mathbf{x}$. The conditional pdf is defined by:

$$p(\mathbf{x}|\mathbf{y}) = \frac{p(\mathbf{x}, \mathbf{y})}{p(\mathbf{y})} \tag{3}$$

with $p(\mathbf{x}, \mathbf{y})$ denoting the *joint pdf* of both random variables $\mathbf{x}$ and $\mathbf{y}$.

4. By writing the pdf $p(\mathbf{x})$ of a random variable $\mathbf{x}$ in form of a *marginal probability density*,

$$p(\mathbf{x}) = \int d\mathbf{y}\, p(\mathbf{x}, \mathbf{y}) = \int d\mathbf{y}\, p(\mathbf{x}|\mathbf{y})\, p(\mathbf{y}), \tag{4}$$

we are able to bring another random variable $\mathbf{y}$ into the play, which might be related to $\mathbf{x}$.

5. By using BAYES *formula* we can calculate how information on $\mathbf{y}$ affects our knowledge on $\mathbf{x}$, provided the pdfs $p(\mathbf{y}|\mathbf{x})$ and $p(\mathbf{x})$ are known. It is a direct consequence of the last two statements and is given by:

$$p(\mathbf{x}|\mathbf{y}) = \frac{p(\mathbf{y}|\mathbf{x})\, p(\mathbf{x})}{\int d\mathbf{x}\, p(\mathbf{y}|\mathbf{x})\, p(\mathbf{x})}. \tag{5}$$

6. *Precise knowledge* that a random variable $\mathbf{x}$ is equal to a certain value $\bar{\mathbf{x}}$ fits well into the description of uncertainty by means of probability densities if Dirac's δ-distributions $p(\mathbf{x}) = \delta(\mathbf{x}; \bar{\mathbf{x}})$ are considered. In this case we have for suitable function $g : \mathbf{x} \mapsto g(\mathbf{x})$ of $\mathbf{x}$: $\mathbb{E}[g(\mathbf{x})] = \int d\mathbf{x}\, g(\mathbf{x})\, \delta(\mathbf{x}; \bar{\mathbf{x}}) = g(\bar{\mathbf{x}})$.

7. An important special case is the GAUSS*ian pdf* characterized by a single maximum concentrated around $\bar{\mathbf{x}}$. Let the quadratic form $q(\mathbf{x}) = \frac{1}{2}(\mathbf{x} - \bar{\mathbf{x}})^\top \mathbf{C}^{-1}(\mathbf{x} - \bar{\mathbf{x}})$ be a measure for the distance between the random variable $\mathbf{x}$ and the 'center' $\bar{\mathbf{x}}$. By $q(\mathbf{x}) = $ const. ellipsoids are defined centered around $\bar{\mathbf{x}}$, whose volume and orientation are determined by a *symmetric and positive definite* matrix $\mathbf{C}$. As a special pdf decaying with an increasing distance of $\mathbf{x}$ from $\bar{\mathbf{x}}$, let us consider $p(\mathbf{x}) = e^{-q(\mathbf{x})} / \int d\mathbf{x}\, e^{-q(\mathbf{x})}$. Evidently, $p(\mathbf{x})$ is positive and correctly normalized. After integration we obtain:

$$p(\mathbf{x}) = \mathcal{N}(\mathbf{x}; \bar{\mathbf{x}}, \mathbf{C}) = \det[2\pi\mathbf{C}]^{-\frac{1}{2}}\, e^{-\frac{1}{2}(\mathbf{x}-\bar{\mathbf{x}})^\top \mathbf{C}^{-1}(\mathbf{x}-\bar{\mathbf{x}})} \tag{6}$$

with an expectation vector and an covariance matrix given by $\mathbb{E}[\mathbf{x}] = \bar{\mathbf{x}}$ and $\mathbb{E}[(\mathbf{x} - \bar{\mathbf{x}})(\mathbf{x} - \bar{\mathbf{x}})^\top] = \mathbf{C}$, respectively. By this, the covariance matrix $\mathbf{C}$ has a simple and intuitive geometrical interpretation. By considering '$\mathbf{C} \rightarrow 0$', a representation of the δ-distribution is defined: $\delta(\mathbf{x}; \bar{\mathbf{x}})$ '=' $\lim_{\text{'}\mathbf{C} \rightarrow 0\text{'}} \mathcal{N}(\mathbf{x}; \bar{\mathbf{x}}, \mathbf{C})$.

8. For GAUSSian pdfs there exists an extremely useful product formula facilitating many calculations:

$$\mathcal{N}(\mathbf{z}; \mathbf{Hx}, \mathbf{R}) \, \mathcal{N}(\mathbf{x}; \mathbf{y}, \mathbf{P}) = \mathcal{N}(\mathbf{z}; \mathbf{Hy}, \mathbf{S}) \, \mathcal{N}(\mathbf{x}; \mathbf{y} + \mathbf{W}(\mathbf{z} - \mathbf{Hy}), \mathbf{P} - \mathbf{WSW}^\top) \tag{7}$$
$$\text{with:} \quad \mathbf{S} = \mathbf{HPH}^\top + \mathbf{R} \quad \text{and} \quad \mathbf{W} = \mathbf{PH}^\top \mathbf{S}^{-1}.$$

This formula can be proven by interpreting $\mathcal{N}(\mathbf{z}; \mathbf{Hx}, \mathbf{R}) \, \mathcal{N}(\mathbf{x}; \mathbf{y}, \mathbf{P})$ as a joint density $p(\mathbf{z}, \mathbf{x}) = p(\mathbf{z}|\mathbf{x})p(\mathbf{x})$. It can be shown that $p(\mathbf{z}, \mathbf{x})$ is a GAUSSian itself:

$$p(\mathbf{z}, \mathbf{x}) = \mathcal{N}\left(\begin{pmatrix} \mathbf{z} \\ \mathbf{x} \end{pmatrix}; \begin{pmatrix} \mathbf{Hy} \\ \mathbf{y} \end{pmatrix}, \begin{pmatrix} \mathbf{S} & \mathbf{HP} \\ \mathbf{PH}^\top & \mathbf{P} \end{pmatrix}\right). \tag{8}$$

Using $p(\mathbf{z}, \mathbf{x})$ and the 'matrix inversion lemma' (e.g. the useful book [10]) calculate the marginal and conditional densities $p(\mathbf{z})$, $p(\mathbf{x}|\mathbf{z})$. Due to $p(\mathbf{z}|\mathbf{x})p(\mathbf{x}) = p(\mathbf{x}|\mathbf{z})p(\mathbf{z})$ the formula is obtained. An equivalent version of the product formula is:

$$\mathcal{N}(\mathbf{z}; \mathbf{Hx}, \mathbf{R}) \, \mathcal{N}(\mathbf{x}; \mathbf{y}, \mathbf{P}) = \mathcal{N}(\mathbf{z}; \mathbf{Hy}, \mathbf{S}) \, \mathcal{N}(\mathbf{x}; \mathbf{Q}^{-1}(\mathbf{P}^{-1}\mathbf{y} + \mathbf{H}^\top \mathbf{R}^{-1}\mathbf{z}), \mathbf{Q}) \tag{9}$$
$$\text{with:} \quad \mathbf{Q} = (\mathbf{P}^{-1} + \mathbf{H}^\top \mathbf{R}^{-1}\mathbf{H})^{-1}.$$

9. Let $\mathbf{x}$ be a GAUSSian random variable. The pdf of $\mathbf{y} = \mathbf{a} + \mathbf{Ax}$ with fixed $\mathbf{a}$ and $\mathbf{A}$ is given by

$$\mathcal{N}(\mathbf{x}; \bar{\mathbf{x}}, \mathbf{X}) \xrightarrow{\mathbf{y} = \mathbf{a} + \mathbf{Ax}} \mathcal{N}(\mathbf{y}; \mathbf{a} + \mathbf{A}\bar{\mathbf{x}}, \mathbf{AXA}^\top). \tag{10}$$

Proof: $p(\mathbf{y}) = \int d\mathbf{x} \, p(\mathbf{x}, \mathbf{y}) = \int d\mathbf{x} \, p(\mathbf{y}|\mathbf{x}) \, p(\mathbf{x}) = \int d\mathbf{x} \, \delta(\mathbf{y}; \mathbf{x}) \, p(\mathbf{x})$ as we have precise knowledge of $\mathbf{y}$ given $\mathbf{x}$ is known. For '$\mathbf{D} \to 0$' we can thus write: $p(\mathbf{y}) = \int d\mathbf{x} \, \mathcal{N}(\mathbf{y}; \mathbf{a} + \mathbf{Ax}, \mathbf{D}) \, \mathcal{N}(\mathbf{x}; \bar{\mathbf{x}}, \mathbf{P}) = \mathcal{N}(\mathbf{y}; \mathbf{a} + \mathbf{A}\bar{\mathbf{x}}, \mathbf{AXA}^\top + \mathbf{D})$ according to the product formula Equation 7.

2.2 Target Tracking: General Problem

Let us consider a time series of measurement sets $Z_l = \{\mathbf{z}_l^1, \ldots, \mathbf{z}_l^{n_k}\}$ related to target states $\mathbf{x}_l$ at instants of time denoted by t_l, $l = 1, \ldots, k$: $\mathcal{Z}^k = \{Z_k, n_k, Z_{k-1}, n_{k-1}, \ldots, Z_1, m_1\} = \{Z_k, n_k, \mathcal{Z}^{k-1}\}$. The individual measurements and the target states be described by vectors $\mathbf{z}_l^j$ and $\mathbf{x}_l$, respectively. In general: $\dim \mathbf{z}_l^j < \dim \mathbf{x}_l$.

The central question of target tracking can be stated as follows: What can be known about the target states $\mathbf{x}_l$ at time instants $t_1, t_2, \ldots, t_{k-1}, t_k, t_{k+1}, \ldots$, i.e. for the past, at present, and in the future, by exploiting the sensor data collected in the times series $\mathcal{Z}^k$?

According to the approach previously sketched, the answer to this question is given by the conditional probability densities $p(\mathbf{x}_l|\mathcal{Z}^k)$, which are to be calculated iteratively. At present we confine the discussion to the case $l = k$; i.e. we are interested in the target states at the current time t_k. Firstly, an application of BAYES' formula yields:

$$p(\mathbf{x}_k|\mathcal{Z}^k) = p(\mathbf{x}_k|Z_k, n_k, \mathcal{Z}^{k-1}) = \frac{p(Z_k, n_k|\mathbf{x}_k, \mathcal{Z}^{k-1}) \, p(\mathbf{x}_k|\mathcal{Z}^{k-1})}{\int d\mathbf{x}_k \, p(Z_k, n_k|\mathbf{x}_k, \mathcal{Z}^{k-1}) \, p(\mathbf{x}_k|\mathcal{Z}^{k-1})}. \tag{11}$$

In many practical cases we will have: $p(Z_k, n_k|\mathbf{x}_k, \mathcal{Z}^{k-1}) = p(Z_k, n_k|\mathbf{x}_k)$. This means that the measurement set at time t_k is depending only on the target state at this time and not on previous measurements. According to Equation 11, the pdf $p(Z_k, n_k|\mathbf{x}_k)$ evidently needs to be known only up to a multiplicative constant: With a function $\ell(Z_k, n_k|\mathbf{x}_k) \propto p(Z_k, n_k|\mathbf{x}_k)$ we obtain the same result. Functions proportional to a conditional probability density in this sense are called *likelihood functions*. The quantities $p(\mathbf{x}_k|\mathcal{Z}^{k-1})$ and $\ell(Z_k, n_k|\mathbf{x}_k)$ in Equation 11 have intuitively clear meanings as sketched in the following subsections.

2.2.1 Target State Prediction

The pdf $p(\mathbf{x}_k|\mathcal{Z}^{k-1})$ is a *prediction* of the target state for the time t_k based on all the measurements received in the past up to and including time t_{k-1}. We can write $p(\mathbf{x}_k|\mathcal{Z}^{k-1})$ as a marginal density in order to bring the target state $\mathbf{x}_{k-1}$ at the previous time t_{k-1} into play:

$$p(\mathbf{x}_k|\mathcal{Z}^{k-1}) = \int d\mathbf{x}_{k-1}\, p(\mathbf{x}_k,\mathbf{x}_{k-1}|\mathcal{Z}^{k-1}) = \int d\mathbf{x}_{k-1}\, \underbrace{p(\mathbf{x}_k|\mathbf{x}_{k-1},\mathcal{Z}^{k-1})}_{\text{target dynamics}}\, \underbrace{p(\mathbf{x}_{k-1}|\mathcal{Z}^{k-1})}_{\text{idea: iteration}}. \tag{12}$$

In many practical cases we can assume $p(\mathbf{x}_k|\mathbf{x}_{k-1},\mathcal{Z}^{k-1}) = p(\mathbf{x}_k|\mathbf{x}_{k-1})$ (MARKOV property). Furthermore a GAUSSian MARKOV dynamics is defined by a GAUSSian *transition density*,

$$p(\mathbf{x}_k|\mathbf{x}_{k-1}) = \mathcal{N}\big(\mathbf{x}_k;\, \mathbf{F}_{k|k-1}\mathbf{x}_{k-1},\, \mathbf{D}_{k|k-1}\big), \tag{13}$$

with an *evolution matrix* $\mathbf{F}_{k|k-1}$ and a *dynamics covariance* matrix $\mathbf{D}_{k|k-1}$ defining the underlying target dynamics model. For a target state $\mathbf{x}_k = (\mathbf{r}_k^\top, \dot{\mathbf{r}}_k^\top, \ddot{\mathbf{r}}_k^\top)^\top$ given by position, velocity, and acceleration vectors in three spatial dimensions the following simple realization is useful in many practical applications [14]:

$$\mathbf{F}_{k|k-1} = \begin{pmatrix} \mathbf{I} & (t_k-t_{k-1})\,\mathbf{I} & \frac{1}{2}(t_k-t_{k-1})^2\,\mathbf{I} \\ \mathbf{O} & \mathbf{I} & (t_k-t_{k-1})\,\mathbf{I} \\ \mathbf{O} & \mathbf{O} & e^{-(t_k-t_{k-1})/\theta}\,\mathbf{I} \end{pmatrix}, \quad \mathbf{D}_{k|k-1} = \Sigma^2(1-e^{-2(t_k-t_{k-1})/\theta}) \begin{pmatrix} \mathbf{O} & \mathbf{O} & \mathbf{O} \\ \mathbf{O} & \mathbf{O} & \mathbf{O} \\ \mathbf{O} & \mathbf{O} & \mathbf{I} \end{pmatrix} \tag{14}$$

with $\mathbf{I} = \text{diag}[1,1,1]$, $\mathbf{O} = \text{diag}[0,0,0]$. According to this simple model, the acceleration $\ddot{\mathbf{r}}_k$ is described by an ergodic MARKOV process with $\mathbb{E}[\ddot{\mathbf{r}}_k] = 0$. The corresponding autocorrelation function decays exponentially and is given by $\mathbb{E}[\ddot{\mathbf{r}}_k\ddot{\mathbf{r}}_l^\top] = \Sigma^2 \exp[-(t_k-t_l)/\theta_t]\,\mathbf{I}$, $l \leq k$. This expression gives a clear meaning to the modeling parameters Σ (*acceleration width*) and θ (*maneuver correlation time*).

2.2.2 Likelihood Function

The likelihood functions $\ell(Z_k,n_k|\mathbf{x}_k)$ describe, what can be learned from the *current* sensor output Z_k,n_k about the current target state $\mathbf{x}_k$. In the special case of well-separated targets, perfect detection, no false returns we have: $n_k = 1$, $Z_k = \{\mathbf{z}_k\}$. With an idealized sensor model describing bias-free measurements by linear functions $\mathbf{H}_k\mathbf{x}_k$ of the target state, which are corrupted by GAUSSian white noise characterized by a measurement error covariance matrix $\mathbf{R}_k$, the likelihood function is given by:

$$\ell(\mathbf{z}_k|\mathbf{x}_k) \propto \mathcal{N}\big(\mathbf{z}_k;\, \mathbf{H}_k\mathbf{x}_k,\, \mathbf{R}_k\big). \tag{15}$$

The possibly time-dependent matrix $\mathbf{H}_k$ is called *measurement matrix* and defines, which characteristic property of the target is currently being measured. At different times the quality of the sensor measurements itself may change as well as the accuracy $\mathbf{R}_k$ by which they are measured.

2.2.3 Combination of Densities

According to these considerations we are in principle able to calculate conditional pdf $p(\mathbf{x}_k|\mathcal{Z}^k)$ iteratively,

$$p(\mathbf{x}_k|\mathcal{Z}^k) = \frac{\ell(Z_k,n_k|\mathbf{x}_k)\,\int d\mathbf{x}_{k-1}\, p(\mathbf{x}_k|\mathbf{x}_{k-1})\, p(\mathbf{x}_{k-1}|\mathcal{Z}^{k-1})}{\int d\mathbf{x}_k\, \ell(Z_k,n_k|\mathbf{x}_k)\,\int d\mathbf{x}_{k-1}\, p(\mathbf{x}_k|\mathbf{x}_{k-1})\, p(\mathbf{x}_{k-1}|\mathcal{Z}^{k-1})}, \tag{16}$$

by combining the following pieces of evidence:

$$\begin{aligned} p(\mathbf{x}_{k-1}|\mathcal{Z}^{k-1}): &\quad \text{available past knowledge} \\ p(\mathbf{x}_k|\mathbf{x}_{k-1}): &\quad \text{target dynamics model} \\ \ell(Z_k,n_k|\mathbf{x}_k): &\quad \text{sensor data, sensor model.} \end{aligned}$$

2.3 A Realization: KALMAN Filter

The well-known KALMAN filter is a straight-forward realization of the general tracking scheme previously sketched in the case of well-separated targets, a GAUSS-MARKOV target dynamics, perfect detection, no false returns. Hence $\mathcal{Z}^k$ is a time series of single measurements: $\mathcal{Z}^k = \{\mathbf{z}_1, \ldots, \mathbf{z}_k\}$. It will become clear below, that in this context GAUSSian pdfs, $p(\mathbf{x}_k|\mathcal{Z}^k) = \mathcal{N}(\mathbf{x}_k; \mathbf{x}_{k|k}, \mathbf{P}_{k|k})$, represent the available knowledge at each time t_k. They are to be calculated iteratively according to the following scheme:

2.3.1 Track Initiation

At the beginning of the iteration the pdf $p(\mathbf{x}_0|\mathcal{Z}^0) = \mathcal{N}(\mathbf{x}_0; \mathbf{x}_{0|0}, \mathbf{P}_{0|0})$ has to describe the initial ignorance. In many cases this is possible by choosing a 'large' covariance matrix $\mathbf{P}_{0|0}$. More strictly speaking, we initialize the interation by $\mathbf{x}_{0|0} = (\mathbf{z}_0, \mathbf{o}, \mathbf{o})^\top$, where $\mathbf{z}_0$ denotes the first measurement, and $\mathbf{P}_0 = \mathrm{diag}[\mathbf{R}_0, (v_{max})^2\mathbf{I}, (q_{max})^2\mathbf{I}]$, respectively. In $\mathbf{P}_{0|0}$ the matrix $\mathbf{R}_0$ is the measurement error covariance matrix of the first measurement $\mathbf{z}_0$, while ignorance about the initial velocity and acceleration is modeled by spheres, whose radius is given by the maximum speed v_{max} and acceleration q_{max}, respectively.

2.3.2 Prediction Step

$$\mathcal{N}(\mathbf{x}_{k-1}; \mathbf{x}_{k-1|k-1}, \mathbf{P}_{k-1|k-1}) \xrightarrow[\mathbf{F}_{k|k-1}, \mathbf{D}_{k|k-1}]{\text{dynamics model}} \mathcal{N}(\mathbf{x}_k; \mathbf{x}_{k|k-1}, \mathbf{P}_{k|k-1}) \tag{17}$$

$$\text{with:} \qquad \mathbf{x}_{k|k-1} = \mathbf{F}_{k|k-1}\mathbf{x}_{k-1|k-1} \tag{18}$$

$$\mathbf{P}_{k|k-1} = \mathbf{F}_{k|k-1}\mathbf{P}_{k-1|k-1}\mathbf{F}_{k|k-1}{}^\top + \mathbf{D}_{k|k-1} \tag{19}$$

These formulae directly result from the elementary probability facts collected in subsection 2.1:

$$p(\mathbf{x}_k|\mathcal{Z}^{k-1}) = \int d\mathbf{x}_{k-1}\, p(\mathbf{x}_k, \mathbf{x}_{k-1}|\mathcal{Z}^{k-1}) = \int d\mathbf{x}_{k-1}\, p(\mathbf{x}_k|\mathbf{x}_{k-1})\, p(\mathbf{x}_{k-1}|\mathcal{Z}^{k-1}) \tag{20}$$

$$= \int d\mathbf{x}_{k-1}\, \underbrace{\mathcal{N}(\mathbf{x}_k; \mathbf{F}_{k|k-1}\mathbf{x}_{k-1}, \mathbf{D}_{k|k-1})}_{\text{dynamics model}}\, \underbrace{\mathcal{N}(\mathbf{x}_{k-1}; \mathbf{x}_{k-1|k-1}, \mathbf{P}_{k-1|k-1})}_{\text{filtering at } t_{k-1}} \tag{21}$$

$$= \mathcal{N}(\mathbf{x}_k; \mathbf{F}_{k|k-1}\mathbf{x}_{k-1|k-1}, \mathbf{F}_{k|k-1}\mathbf{P}_{k-1|k-1}\mathbf{F}_{k|k-1}{}^\top + \mathbf{D}_{k|k-1}) \underbrace{\int d\mathbf{x}_{k-1}\, \mathcal{N}(\mathbf{x}_{k-1}; \mathbf{b}, \mathbf{B})}_{=1 \quad \text{(normalization)}}.$$

In the last step we made use of the product formula for GAUSSians (Equation 7).

2.3.3 Filtering Step

$$\mathcal{N}(\mathbf{x}_k; \mathbf{x}_{k|k-1}, \mathbf{P}_{k|k-1}) \xrightarrow[\text{sensor model: } \mathbf{H}_k, \mathbf{R}_k]{\text{current measurement } \mathbf{z}_k} \mathcal{N}(\mathbf{x}_k; \mathbf{x}_{k|k}, \mathbf{P}_{k|k}) \tag{22}$$

$$\text{with:} \qquad \begin{aligned} \mathbf{x}_{k|k} &= \mathbf{x}_{k|k-1} + \mathbf{W}_{k|k-1}(\mathbf{z}_k - \mathbf{H}_k\mathbf{x}_{k|k-1}), & \mathbf{W}_{k|k-1} &= \mathbf{P}_{k|k-1}\mathbf{H}_k{}^\top \mathbf{S}_{k|k-1}{}^{-1} \\ \mathbf{P}_{k|k} &= \mathbf{P}_{k|k-1} - \mathbf{W}_{k|k-1}\mathbf{S}_{k|k-1}\mathbf{W}_{k|k-1}^\top, & \mathbf{S}_{k|k-1} &= \mathbf{H}_k\mathbf{P}_{k|k-1}\mathbf{H}_k{}^\top + \mathbf{R}_k. \end{aligned} \tag{23}$$

Also these formulae directly result from elementary probability reasoning (subsection 2.1) and an application of the product formula (Equation 7):

$$p(\mathbf{x}_k|\mathcal{Z}^k) = p(\mathbf{x}_k|\mathbf{z}_k, \mathcal{Z}^{k-1}) = \frac{p(\mathbf{z}_k|\mathbf{x}_k)\, p(\mathbf{x}_k|\mathcal{Z}^{k-1})}{\int d\mathbf{x}_k\, p(\mathbf{z}_k|\mathbf{x}_k)\, p(\mathbf{x}_k|\mathcal{Z}^{k-1})} \qquad \text{(BAYES' rule)} \tag{24}$$

$$= \frac{\mathcal{N}(\mathbf{z}_k; \mathbf{H}_k\mathbf{x}_k, \mathbf{R}_k)\, \mathcal{N}(\mathbf{x}_k; \mathbf{x}_{k|k-1}, \mathbf{P}_{k|k-1})}{\int d\mathbf{x}_k\, \underbrace{\mathcal{N}(\mathbf{z}_k; \mathbf{H}_k\mathbf{x}_k, \mathbf{R}_k)}_{\text{likelihood function}}\, \underbrace{\mathcal{N}(\mathbf{x}_k; \mathbf{x}_{k|k-1}, \mathbf{P}_{k|k-1})}_{\text{prediction at } t_k}}. \tag{25}$$

2.3.4 Retrodiction

$$\mathcal{N}(\mathbf{x}_l;\, \mathbf{x}_{l|k},\, \mathbf{P}_{l|k}) \xleftarrow[\text{prediction output}]{\text{filtering output}} \mathcal{N}(\mathbf{x}_{l+1};\, \mathbf{x}_{l+1|k},\, \mathbf{P}_{l+1|k}) \tag{26}$$

$$\text{with:} \quad \begin{aligned} \mathbf{x}_{l|k} &= \mathbf{x}_{l|l} + \mathbf{W}_{l|l+1}(\mathbf{x}_{l+1|k} - \mathbf{x}_{l+1|l}) \qquad \mathbf{W}_{l|l+1} = \mathbf{P}_{l|l}\mathbf{F}_{l+1|l}^{\top}\mathbf{P}_{l+1|l}^{-1}, \\ \mathbf{P}_{l|k} &= \mathbf{P}_{l|l} + \mathbf{W}_{l|l+1}(\mathbf{P}_{l+1|k} - \mathbf{P}_{l+1|l})\mathbf{W}_{l|l+1}^{\top} \end{aligned} \tag{27}$$

These update equations are also called RAUCH-TUNG-STRIEBEL formulae and result from the following considerations:

$$p(\mathbf{x}_l|\mathcal{Z}^k) = \int d\mathbf{x}_{l+1}\, p(\mathbf{x}_l, \mathbf{x}_{l+1}|\mathcal{Z}^k)\, p(\mathbf{x}_{l+1}|\mathcal{Z}^k) = \int d\mathbf{x}_{l+1}\, p(\mathbf{x}_l|\mathbf{x}_{l+1}, \mathcal{Z}^k)\, p(\mathbf{x}_{l+1}|\mathcal{Z}^k)$$
$$= \int d\mathbf{x}_{l+1}\, p(\mathbf{x}_l|\mathbf{x}_{l+1}, \mathcal{Z}^k)\, \underbrace{\mathcal{N}(\mathbf{x}_{l+1};\, \mathbf{x}_{l+1|k},\, \mathbf{P}_{l+1|k})}_{\text{retrodiction at } t_{l+1}} \tag{28}$$

with $p(\mathbf{x}_l|\mathbf{x}_{l+1}, \mathcal{Z}^k)$ given by

$$p(\mathbf{x}_l|\mathbf{x}_{l+1}, \mathcal{Z}^k) = \frac{p(\mathbf{x}_{l+1}|\mathbf{x}_l)\, p(\mathbf{x}_l|\mathcal{Z}^l)}{\int d\mathbf{x}_l\, p(\mathbf{x}_{l+1}|\mathbf{x}_l)\, p(\mathbf{x}_l|\mathcal{Z}^l)} = \frac{\mathcal{N}(\mathbf{x}_{l+1};\, \mathbf{F}_{l+1|l}\mathbf{x}_l,\, \mathbf{D}_{l+1|l})\, \mathcal{N}(\mathbf{x}_l;\, \mathbf{x}_{l|l},\, \mathbf{P}_{l|l})}{\int d\mathbf{x}_l\, \underbrace{\mathcal{N}(\mathbf{x}_{l+1};\, \mathbf{F}_{l+1|l}\mathbf{x}_l,\, \mathbf{D}_{l+1|l})}_{\text{dynamics model}}\, \underbrace{\mathcal{N}(\mathbf{x}_l;\, \mathbf{x}_{l|l},\, \mathbf{P}_{l|l})}_{\text{filtering at time } t_l}}. \tag{29}$$

An application of the product formulae in Equation 29, insertion of the result into Equation 28, and a second use of the product formulae yields the retrodiction update formulae in Equation 27.

2.3.5 Discussion

We discuss some characteristic properties of KALMAN filtering and RAUCH-TUNG-STRIEBEL retrodiction:

- The KALMAN filter algorithm is linear in the sensor data, i.e. the superposition principle is valid.

- The conditional pdfs are fully characterized by the related expectations and covariance matrices.

- KALMAN filtering corrects predictions by the difference between actual and expected measurements.

- Variable revisit intervals as well as time-dependent dynamics and sensor models are inherently admitted.

- The computational effort is rather small; matrix inversions involved can often be performed analytically.

- Qualitatively speaking, the retrodicted densities $p(\mathbf{x}_l|\mathcal{Z}^k)$ are 'sharper' than $p(\mathbf{x}_k|\mathcal{Z}^k)$ and $p(\mathbf{x}_l|\mathcal{Z}^l)$.

- For retrodiction only expectations and covariance matrices of the filtering and predictions are used.

- The sensor data themselves are processed in the filtering step only and not needed in retrodiction.

- The information gain by retrodiction is driven by the target dynamics: $\mathbf{W}_{l|l+1} = \mathbf{P}_{l|l}\mathbf{F}_{l+1|l}^{\top}\mathbf{P}_{l+1|l}^{-1}$.

- There is no gain by retrodiction at present: Tracks are 'smoothed' at the expense of some delay.

- Retrodiction has potential applications for target classification/identification/IFF from track data.

2.3.6 Non-linearities

In a radar system typically target range, azimuth, range-rate, and eventually target elevation are measured. These quantities are easily described in a polar coordinate system, while for modeling the target dynamics Cartesian coordinates better suited. Therefore, it seems to be convenient to perform the prediction step of the density update in the Cartesian dynamics system and the filtering in sensor coordinates according to the following scheme:

$$
\begin{array}{ll}
\text{dynamics system:} & \\
\mathbf{x}^d = (x, y, \dot{x}, \dot{y}) & p(\mathbf{x}^d_{k-1} \mid \mathcal{Z}^{k-1}) \xrightarrow[\text{dynamics}]{p(\mathbf{x}^d_k \mid \mathbf{x}^d_{k-1})} p(\mathbf{x}^d_k \mid \mathcal{Z}^{k-1}) \qquad\qquad p(\mathbf{x}^d_k \mid \mathcal{Z}^k) \\[2mm]
& \qquad\quad \uparrow \mathbf{t}_{d \leftarrow s} \qquad\qquad\qquad\quad \downarrow \mathbf{t}_{s \leftarrow d} \qquad\qquad\qquad\qquad \uparrow \mathbf{t}_{d \leftarrow s} \\[2mm]
\text{sensor system:} & \\
\mathbf{x}^s = (r, \varphi, \dot{r}, \dot{\varphi}) & p(\mathbf{x}^s_{k-1} \mid \mathcal{Z}^{k-1}) \qquad\qquad\qquad p(\mathbf{x}^s_k \mid \mathcal{Z}^{k-1}) \xrightarrow[\text{sensor}]{p(\mathbf{z}_k \mid \mathbf{x}^s_k)} p(\mathbf{x}^s_k \mid \mathcal{Z}^k)
\end{array}
\tag{30}
$$

$$
\text{scan } k-1 \qquad\qquad\qquad\qquad\qquad \text{scan } k \qquad\qquad\qquad\qquad \text{scan } k
$$

The corresponding coordinate transformations $\mathbf{t}_{d \leftarrow s}$ and $\mathbf{t}_{s \leftarrow d}$, however, are non-linear and given by:

$$
\mathbf{t}_{d \leftarrow s}[\mathbf{x}^s] = \begin{pmatrix} x \\ y \\ \dot{x} \\ \dot{y} \end{pmatrix} = \begin{pmatrix} r \cos \varphi \\ r \sin \varphi \\ \dot{r} \cos \varphi - r \dot{\varphi} \sin \varphi \\ \dot{r} \sin \varphi + r \dot{\varphi} \cos \varphi \end{pmatrix}, \qquad
\mathbf{t}_{s \leftarrow d}[\mathbf{x}^d] = \begin{pmatrix} r \\ \varphi \\ \dot{r} \\ \dot{\varphi} \end{pmatrix} = \begin{pmatrix} \sqrt{x^2 + y^2} \\ \arctan y/x \\ (x\dot{x} + y\dot{y})/\sqrt{x^2 + y^2} \\ (x\dot{y} - y\dot{x})/(x^2 + y^2) \end{pmatrix}.
\tag{31}
$$

This non-linear character of the coordinate transformations in particular implies that a GAUSSian pdf $p(\mathbf{x}^s_{k-1} \mid \mathcal{Z}^{k-1})$ is no longer a GAUSSian after its transformation into the dynamics system and vice versa. In order to circumvent this problem in 'extended' KALMAN filtering the non-linear transformations are simply linearized by a first order Taylor expansion around the filtering $\mathbf{x}^s_{k|k}$ in the sensor system or around the prediction $\mathbf{x}^d_{k|k-1}$ in the dynamics system, respectively:

$$
\mathbf{t}_{d \leftarrow s}[\mathbf{x}^s_k] \approx \mathbf{t}_{d \leftarrow s}[\mathbf{x}^s_{k|k}] + \mathbf{T}_{d \leftarrow s}[\mathbf{x}^s_{k|k}] \, (\mathbf{x}^s_k - \mathbf{x}^s_{k|k}) \qquad \text{with:} \qquad \mathbf{T}_{d \leftarrow s} = \partial \mathbf{t}_{d \leftarrow s}[\mathbf{x}^s_{k|k}]/\partial \mathbf{x}^s_{k|k}
\tag{32}
$$

$$
\mathbf{t}_{s \leftarrow d}[\mathbf{x}^d_k] \approx \mathbf{t}_{s \leftarrow d}[\mathbf{x}^d_{k|k-1}] + \mathbf{T}_{d \leftarrow s}[\mathbf{x}^d_{k|k-1}] \, (\mathbf{x}^d_k - \mathbf{x}^d_{k|k-1}) \qquad \mathbf{T}_{s \leftarrow d} = \partial \mathbf{t}_{d \leftarrow s}[\mathbf{x}^d_{k|k-1}]/\partial \mathbf{x}^d_{k|k-1}.
\tag{33}
$$

With this approximation the 'GAUSSianity' of the densities is preserved according to Equation 10 describing the pdf of an affine transform of a GAUSSian random variable.

Let us consider a more simplified situation, where only range and azimuth measurements are available. These measurements $\mathbf{z}_k = (r_k, \varphi_k)^\top$ are characterized by a diagonal measurement error covariance matrix $\mathbf{R}^p = \mathrm{diag}[\sigma_r^2, \sigma_\varphi^2]$ assuming that range and azimuth measurements are independent from each other. When the measurements $\mathbf{z}_k$ are transformed into Cartesian coordinates, the corresponding measurement error covariance matrix can approximately be obtained as follows: Let us expand $\mathbf{t}[\mathbf{z}_k]$ around the prediction $\mathbf{x}_{k|k-1}$:

$$
\mathbf{t}[\mathbf{z}_k] = (r_k \cos \varphi_k, \sin \varphi_k)^\top \approx \mathbf{t}[\mathbf{x}_{k|k-1}] + \mathbf{T}_{k|k-1} \, (\mathbf{z}_k - \mathbf{x}_{k|k-1}),
\tag{34}
$$

where the corresponding Jacobi matrix can be written as the product of a rotation and a dilation:

$$
\mathbf{T}_{k|k-1} = \frac{\partial \mathbf{t}[\mathbf{x}_{k|k-1}]}{\partial \mathbf{x}_{k|k-1}} = \begin{pmatrix} \cos \varphi_{k|k-1} & -r_{k|k-1} \sin \varphi_{k|k-1} \\ \sin \varphi_{k|k-1} & r_{k|k-1} \cos \varphi_{k|k-1} \end{pmatrix} = \underbrace{\begin{pmatrix} \cos \varphi_{k|k-1} & -\sin \varphi_{k|k-1} \\ \sin \varphi_{k|k-1} & \cos \varphi_{k|k-1} \end{pmatrix}}_{\text{rotation } \mathbf{D}_\varphi} \underbrace{\begin{pmatrix} 1 & 0 \\ 0 & r_{k|k-1} \end{pmatrix}}_{\text{dilation } \mathbf{S}_r}.
\tag{35}
$$

According to Equation 10 the measurement error covariance in Cartesian coordinate is depending on time (i.e. on the predicted target range $r_{k|k-1}$ and azimuth $\varphi_{k|k-1}$) as well as on the underlying sensor-to-target

geometry. It is given by:

$$\mathbf{R}_k^c = \mathbf{T}_{k|k-1}\mathbf{R}^p\mathbf{T}_{k|k-1}^\top = \mathbf{D}_\varphi\mathbf{S}_r\,\mathbf{R}^p\,\mathbf{S}_r D_\varphi^\top = \mathbf{D}_\varphi \begin{pmatrix} \sigma_r^2 & 0 \\ 0 & (r_{k|k-1}\sigma_\varphi)^2 \end{pmatrix} \mathbf{D}_\varphi^\top. \tag{36}$$

As a direct consequence, the Cartesian measurement error ellipses typically increase with increasing range. In certain applications it may be useful to deal with different measurement accuracies, depending on the tracking task under consideration, such as search, acquisition, or high-precision tracking for phased-array radar [4].

There exist more advanced methods for dealing with non-linearities such as "particle filtering" or "unscented KALMAN update equations yield in this case:

Initiation: $\qquad \mathbf{x}_{1|1} \quad = \mathbf{z}_1$

Prediction: $\qquad \mathbf{x}_{k|k-1} \quad = \mathbf{x}_{k-1|k-1}, \mathbf{P}_{k|k-1} = \mathbf{P}_{k-1|k-1}, \quad k = 2, 3, \ldots$

Filtering: $\qquad \begin{aligned} \mathbf{x}_{k|k} \quad &= \mathbf{x}_{k-1|k-1} + \mathbf{W}_{k-1}\,(\mathbf{z}_k - \mathbf{x}_{k-1|k-1}) = \mathbf{P}_{k|k}\big(\mathbf{R}_k^{-1}\mathbf{z}_k + \mathbf{P}_{k-1|k-1}^{-1}\mathbf{x}_{k-1|k-1}\big) \\ &= \mathbf{P}_{k|k} \sum_{i=1}^k \mathbf{R}_i^{-1}\mathbf{z}_i \end{aligned}$

$\qquad \begin{aligned} \mathbf{P}_{k|k} \quad &= \mathbf{P}_{k-1|k-1} - \mathbf{W}_{k-1}\big(\mathbf{P}_{k-1|k-1} + \mathbf{R}_k\big)\mathbf{W}_{k-1}^\top \\ &= \mathbf{P}_{k-1|k-1} - \mathbf{P}_{k-1|k-1}(\mathbf{P}_{k-1|k-1} + \mathbf{R}_k)^{-1}\mathbf{P}_{k-1|k-1} = (\mathbf{P}_{k-1|k-1}^{-1} + \mathbf{R}_k^{-1})^{-1} \\ &= \big(\sum_{i=1}^k \mathbf{R}_i^{-1}\big)^{-1}. \end{aligned}$

In the last step we made use of the matrix inversion lemma. From these considerations it becomes clear that in case of stationary targets the KALMAN filter is equivalent to a weighted, recursive arithmetic mean of the sensor data. The related error covariance matrix is a harmonic mean of the corresponding measurement error covariance matrices. We collect some observations:

- If all measurement covariances R_i, $i = 1, \ldots, k$ are identical, we observe the expected 'square-root' law:

$$P_{k|k} = R/k. \tag{37}$$

- If all measurement error ellipses involved differ significantly in the geometrical orientation relative to each other, a much larger effect can be observed.

- The 'statistical intersection' of error ellipses is described by calculating the *harmonic mean* of the related error covariance matrices:

$$\sum_{i=1}^k \mathbf{R}_i^{-1}\mathbf{z}_i. \tag{38}$$

- In the limiting case of very narrow measurement error ellipses the triangulation of the target position from bearings is obtained ($\rightarrow$ multiple sensor data fusion).

- These considerations are also valid in 3D and for more abstract measurements.

Let us consider an example: The target position in Cartesian coordinates be given by $\mathbf{r} = r[\cos(\frac{\pi}{4}), \sin(\frac{\pi}{4})]^\top = r/\sqrt{2}(1, 1)^\top$. The measurement error covariances of sensor 1 and 2 is given by $\mathbf{R}_1 =$

$\mathbf{D}_1\mathbf{S}\mathbf{D}_1^\top$ and $\mathbf{R}_2 = \mathbf{D}_2\mathbf{S}\mathbf{D}_2^\top$ with $\mathbf{D}_1 = \mathbf{D}(\frac{\pi}{4}) = \frac{1}{\sqrt{2}}\left(\begin{smallmatrix} 1 & -1 \\ 1 & 1 \end{smallmatrix}\right)$, $\mathbf{D}_2 = \mathbf{D}(\frac{3\pi}{4}) = \frac{1}{\sqrt{2}}\left(\begin{smallmatrix} 1 & 1 \\ -1 & 1 \end{smallmatrix}\right)$, $\mathbf{S} = \text{diag}[\sigma_r^2, (r\sigma_\varphi)^2]$. We hence obtain the 'fused' measurement error covariance

$$\mathbf{R}^{-1} = \mathbf{R}_1^{-1} + \mathbf{R}_2^{-1} = \mathbf{D}_1^\top\mathbf{S}^{-1}\mathbf{D}_1 + \mathbf{D}_2^\top\mathbf{S}^{-1}\mathbf{D}_2 = \mathbf{D}_1^\top(\mathbf{S}^{-1} + \mathbf{D}_1\mathbf{D}_2^\top\mathbf{S}^{-1}\mathbf{D}_2\mathbf{D}_1^\top)\mathbf{D}_1 \tag{39}$$

$$= \mathbf{D}_1^\top\begin{pmatrix} \sigma_r^{-2}+(r\sigma_\varphi)^{-2} & 0 \\ 0 & \sigma_r^{-2}+(r\sigma_\varphi)^{-2} \end{pmatrix}\mathbf{D}_1 \tag{40}$$

That means $\mathbf{R}$ is a sphere with radius Σ given by $\frac{1}{\Sigma^2} = \frac{1}{\sigma_r^2} + \frac{1}{(r\sigma_\varphi)^2}$. Let us consider the following special cases: 'triangulation' $(\sigma_r \gg r\sigma_\varphi) \to R = (r\sigma_\varphi)^2$, 'large distance' $(r \gg \sigma_r/\sigma_\varphi) \to R = \sigma_r^2$.

A practically important problem is the following: If there are more than one target in the common field of view of both sensors, not every intersection of bearing beams actually corresponds to a real target position. For more details and possible solutions of resulting "deghosting problem" see [1, 2].

2.3.7 Expectation Gates

KALMAN filtering provides also the means for calculating the statistical properties of *expected* measurements. The corresponding pdf is itself the basis for calculating an expectation gate containing an expected measurement with a given probability (*correlation probability* P_c). The conditional pdf of an expected measurement $\mathbf{z}_k$ at time t_k given the accumulated sensor data up to and including the time t_{k-1} can be calculated by:

$$p(\mathbf{z}_k | \mathcal{Z}^{k-1}) = \int d\mathbf{x}_k\, p(\mathbf{z}_k, \mathbf{x}_k | \mathcal{Z}^{k-1}) = \int d\mathbf{x}_k\, p(\mathbf{z}_k|\mathbf{x}_k)\, p(\mathbf{x}_k|\mathcal{Z}^{k-1}) \tag{41}$$

$$= \int d\mathbf{x}_k\, \underbrace{\mathcal{N}(\mathbf{z}_k; \mathbf{H}_k\mathbf{x}_k, \mathbf{R}_k)}_{\text{likelihood: sensor model}}\, \underbrace{\mathcal{N}(\mathbf{x}_k; \mathbf{x}_{k|k-1}, \mathbf{P}_{k|k-1})}_{\text{prediction for time } t_k} \tag{42}$$

$$= \mathcal{N}(\mathbf{z}_k; \mathbf{H}_k\mathbf{x}_{k|k-1}, \mathbf{S}_{k|k-1}) \quad \text{with:} \quad \mathbf{S}_{k|k-1} = \mathbf{H}_k\mathbf{P}_{k|k-1}\mathbf{H}_k^\top + \mathbf{R}_k \tag{43}$$

according to the product formula (Equation 7). Evidently, $\mathbf{v}_{k|k-1} = \mathbf{z}_k - \mathbf{H}_k\mathbf{x}_{k|k-1}$ is a GAUSSian random variable with zero expectation and the covariance matrix $\mathbf{S}_{k|k-1}$. Being the difference between actual and expected measurement, it is called *innovation*, $\mathbf{S}_{k|k-1}$ is thus referred to as *innovation covariance*. By

$$||\mathbf{v}_{k|k-1}||^2 = \mathbf{v}_{k|k-1}^\top\mathbf{S}_{k|k-1}^{-1}\mathbf{v}_{k|k-1} \le \lambda(P_c) \tag{44}$$

an ellipsoid is defined, which contains the target measurement $\mathbf{z}_k$ with probability P_c. The actual size of the *gate parameter* $\lambda(P_c)$ for a given value of P_c can be taken from a χ^2-table [4].

3 Elements of Multiple Hypothesis Tracking

As an example let us consider 6 sensor reports produced by two closely-spaced targets at time t_k (Figure 5). This single frame of observations is by no means uniquely interpretable. Among other *feasible interpretation hypotheses* the black dots could be assumed to represent real position measurements of the targets, while all other plots are false (Figure 5a). The asterisks indicate the predicted target positions provided by the tracking system. Under the statistical assumptions previously discussed, the expected target measurements are normally distributed about their predictions with a covariance matrix $\mathbf{S}_{k|k-1}$ determined by the related state prediction covariance and the measurement error. As any prediction uses assumptions on the underlying system dynamics, both the sensor performance and the dynamics model enter into the statistics of the expected target measurements. A natural scalar measure for the deviation between the predicted and an actually received measurement is given by $||\mathbf{v}_{k|k-1}||^2 = \mathbf{v}_{k|k-1}^\top\mathbf{S}_{k|k-1}^{-1}\mathbf{v}_{k|k-1}$, also called *Mahalanobis norm*. *Gating* means that only those sensor returns are considered for track maintenance, whose innovations are smaller than a certain predefined threshold $\lambda(P_c)$.

(a) two resolved targets   (b) two unresolved targets
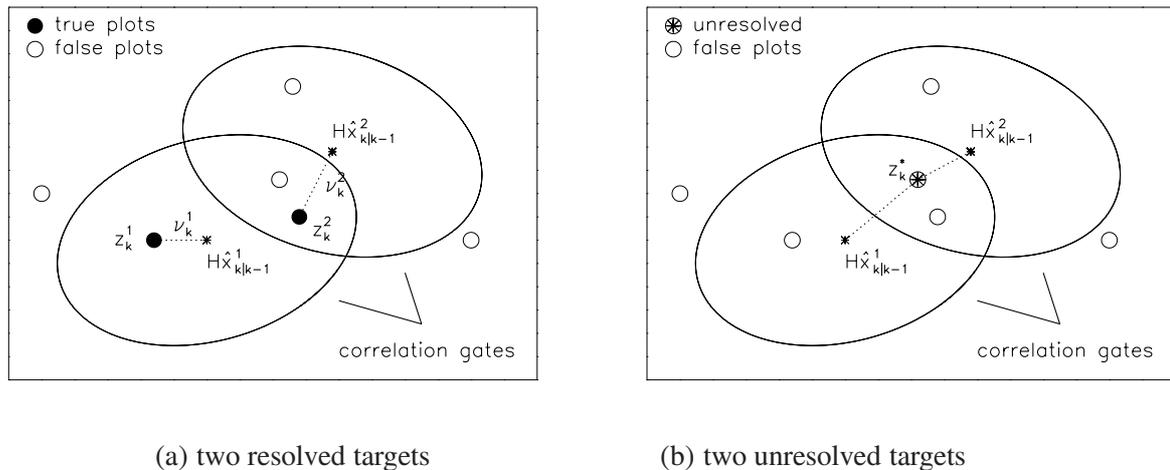
Figure 5: Sensor Data of Uncertain Origin with Competing Interpretations

Competing with the previously discussed data interpretation, however, there exist many other feasible association hypotheses; for instance, the targets could have produced a single unresolved measurement as indicated in Figure 5b, all other plots being false returns. Alternatively, one of both targets might not have been detected or no target detection might have occurred at all, the gates containing false returns only. The correlation gates and thus the ambiguity of the received sensor data are the larger the more false returns and missed detections or even successively missed detections must be taken into account, if the measurement errors involved or the data innovation intervals are large, or if uncertainty regarding the target dynamics model or agile targets exists. As will become clear below, the innovation statistics related to a particular interpretation hypothesis is essential to evaluating its statistical weight.

3.1 Ad-hoc Approaches

For dealing with sensor data of uncertain origin several well-established ad-hoc methods exist which are implemented in numerous operational tracking systems. Under benign conditions *gating* can be sufficient for separating real target measurements from competing sensor returns. The resulting plot is then processed by KALMAN filtering or one of its derivatives. In the previous example (Figure 5) two sensor reports can be excluded by this measure. Evidently, the gate must be sufficiently large, otherwise the real plot might be excluded from processing. By *Nearest Neighbor* (NN) filters [4] only the measurement having the smallest innovation is processed via KALMAN filtering if competing returns exist in the gates. This approach fails, however, if one of the interpretation hypotheses indicated in Figure 5 is true. (Joint) *Probabilistic Data Association* (PDA, JPDA) filters [3] are adaptive mono-hypothesis trackers that show data-driven adaptivity in case of data association conflicts as will be discussed below.

A more rigorous Bayesian approach, capable of handling challenging conditions as sketched in the introduction, leads to *Multiple Hypothesis Tracking* (MHT) discussed below [16]. The ad-hoc methods mentioned (KF, NN, PDAF, JPDAF) quite naturally prove to be limiting cases of this more general approach.

3.2 Sensor Modeling

A statistical description of what kind of information is provided by the sensor systems is prerequisite to processing of the n_k sensor output data $Z_k = \{\mathbf{z}_k^j\}_{j=1}^{n_k}$ consecutively received at discrete instants of time t_k. For the sake of simplicity, our discussion and terminology is confined to point-source objects, small extended objects, possibly unresolved closely-spaced objects, or small clusters of such objects; i.e. we consider "small

targets" following Oliver Drummond's definition [8]. The underlying statistical models essentially determine the feasible interpretations of the received sensor reports.

3.2.1 Detection Process

The detection process is essentially a means of rata rate reduction and therefore prior to any further sensor signal processing which results in sensor reports possibly related to objects of interest.

For resolved objects and a given association hypothesis each sensor return can be associated to exactly one individual object, whereas for unresolved closely-spaced targets a given report may correspond to several objects. It is, thus, reasonable to introduce different detection probabilities for resolved and unresolved objects: P_D, P_D^u. Moreover, the detection process and the production of measurements (fine localization by monopulse processing, for instance [5, p. 119 ff.]) are assumed to be statistically independent.

Let FoV (Field of View) denote a region large enough to contain all relevant sensor reports at scan k. False detections or detections produced by unwanted objects are assumed to be equally distributed in FoV and independent from scan to scan. Moreover let the number of false returns in FoV be Poisson-distributed according to the distribution

$$p_F(n_k) = \frac{1}{n_k!} \, (|\text{FoV}| \, \rho_F)^{n_k} \, e^{-|\text{FoV}| \rho_F}, \tag{45}$$

where |FoV| denotes the volume of FoV and ρ_F the spatial false return density.

In a typical radar application a simple quadrature detector decides on target detection if the received signal strength exceeds a certain threshold: $a_k^2 > \lambda_D$. For a given fluctuation model of the radar cross section of the targets, the detection probability depends on the signal-to-noise ratio of the sensor and the detector threshold, while the false alarm probability is a function of the detector threshold alone. Provided the received signal strength is accessible for the tracking system, it can be used as input information for adaptive threshold control [4], for discriminating of false returns [12, 13] or for phased-array energy management [19]. A more detailed discussion will be given in the second talk (subsection 1.2.4).

3.2.2 Measurements

For a resolved object let $\mathbf{z}_k$ be a bias-free measurement of its kinematical state vector $\mathbf{x}_k$ at time t_k with an additive, normally distributed measurement error:

$$\mathbf{z}_k = \mathbf{H}_k \mathbf{x}_k + \mathbf{w}_k, \; \mathbf{w}_k \sim N(0, \mathbf{R}_k) \quad \longleftrightarrow \quad p(\mathbf{z}_k|\mathbf{x}_k) = \mathcal{N}(\mathbf{z}_k; \mathbf{H}_k \mathbf{x}_k, \mathbf{R}_k) \tag{46}$$

as before in the case of KALMAN filtering. In case of a non-linear relationship between the target state and the measurement, $\mathbf{z}_k = \mathbf{h}_k(\mathbf{x}_k)$, we thus have to deal with data-dependent measurement matrices.

In case of a resolution conflict we interpret an unresolved plot $\mathbf{z}_k^g$ at time t_k as a measurement of the group center [20], i.e.

$$\mathbf{z}_k^g = \mathbf{H}_g \mathbf{x}_k + \mathbf{u}_k^g \qquad \text{with} \quad \mathbf{H}_g \mathbf{x}_k = \tfrac{1}{2} \mathbf{H}(\mathbf{x}_k^1 + \mathbf{x}_k^2), \tag{47}$$

where $\mathbf{u}_k^g \sim N(0, \mathbf{R}_g)$ denotes the measurement error characterized by a corresponding group measurement error covariance matrix $\mathbf{R}_g$ [20]. Let $\mathbf{H}$ be the underlying measurement matrix defined by $\mathbf{H}\mathbf{x}_k^i = (r_k^i, \varphi_k^i)$.

Monopulse angle estimation techniques provide approximately bias-free, normally distributed angular measurements. While in principle high precision monopulse measurements are available also in range, in many radar systems the range measurement errors are a superposition of errors uniformly distributed in the related range cells. For convenience and without significant degradation of the tracking process, however, in many cases range measurement errors can be assumed normally distributed with a standard deviation σ_r which must not be chosen too optimistically. For a more detailed discussion see [4][chapter 2].

3.2.3 Sensor Resolution

We expect that the resolution performance of the sensor strongly depends on the current sensor-to-group geometry and the relative orientation of the targets within the group. For physical reasons the resolution in range and azimuth will be independent from each other. The sensor's resolution capability also depends on the particular signal processing used and on the random target fluctuations. As a complete description is rather complicated, we are looking for a simplified, but qualitatively correct and mathematically tractable model.

In any case the resolution capability in range and azimuth is limited by the band- and beam-width of the sensor characterized by the parameters α_r, α_φ. These radar specific parameters must explicitly enter into any processing of possibly unresolved plots.

Resolution phenomena will be observed if the range and angular distances are small compared with α_r, α_φ: $\Delta r / \alpha_r < 1$, $\Delta \varphi / \alpha_\varphi < 1$. The targets within the group are resolvable if $\Delta r / \alpha_r \gg 1$, $\Delta \varphi / \alpha_\varphi \gg 1$. Furthermore we expect a narrow transient region. A more quantitative description is provided by introducing a resolution probability $P_r = P_r(\Delta r, \Delta \varphi)$ depending on the sensor-to-group geometry. It can be expressed by a corresponding probability of being unresolvable P_u. Let us describe P_u by a Gaussian-type function of the relative range and angular distances [20]:

$$P_r(\Delta r, \Delta \varphi) = 1 - P_u(\Delta r, \Delta \varphi) \tag{48}$$

$$\text{with} \quad P_u(\Delta r, \Delta \varphi) = \exp\left[-\log 2 (\tfrac{\Delta r}{\alpha_r})^2\right] \exp\left[-\log 2 (\tfrac{\Delta \varphi}{\alpha_\varphi})^2\right]. \tag{49}$$

Evidently, this simple model for describing resolution phenomena reflects the previous, more qualitative discussion. We in particular observe that P_u is reduced by a factor of 2 if Δr is increased from zero to α_r. Due to the Gaussian character of its dependency on the state vector $\mathbf{x}_k$ the probability P_u can be written in terms of a normal density:

$$P_u = \exp\left[-\log 2 \, [(r_k^1 - r_k^2)/\alpha_r]^2\right] \exp\left[-\log 2 \, [(\varphi_k^1 - \varphi_k^2)/\alpha_\varphi]^2\right] \tag{50}$$

$$= \exp\left[-\log 2 \, (\mathbf{H}\mathbf{x}_k^1 - \mathbf{H}\mathbf{x}_k^2)^\top \mathbf{A}^{-1}(\mathbf{H}\mathbf{x}_k^1 - \mathbf{H}\mathbf{x}_k^2)\right] \tag{51}$$

$$= \exp\left[-\log 2 \, (\mathbf{H}_u\mathbf{x}_k)^\top \mathbf{A}^{-1}\mathbf{H}_u\mathbf{x}_k\right]. \tag{52}$$

Here the *resolution matrix* $\mathbf{A}$ is defined by $\mathbf{A} = \mathbf{diag}(\alpha_r^2, \alpha_\varphi^2)$, while the quantity $\mathbf{H}_u\mathbf{x}_k = \mathbf{H}(\mathbf{x}_k^1 - \mathbf{x}_k^2)$ can be interpreted a measurement matrix for distance measurements.

Up to a constant factor the resolution probability probability $P_u(\mathbf{x}_k)$ might formally be interpreted as the ficticious likelihood function of a measurement 0 of the distance $\mathbf{H}(\mathbf{x}_k^1 - \mathbf{x}_k^2)$ between the targets with a corresponding *ficticious* measurement error covariance matrix $\mathbf{R}_u$ defined by the resolution parameters α_r, α_φ.

$$P_u(\mathbf{x}_k) = |2\pi\mathbf{R}_u|^{-1/2} \, \mathcal{N}\big(\mathbf{O}; \mathbf{H}_u\mathbf{x}_k, \mathbf{R}_u\big) \tag{53}$$

$$\text{with} \quad \mathbf{R}_u = \frac{\mathbf{A}}{2\log 2} = \tfrac{1}{2\log 2}\mathrm{diag}[\alpha_r^2, \alpha_\varphi^2]. \tag{54}$$

According to a first order Taylor expansion around the predicted range $r_{k|k-1}^g$ and azimuth $\varphi_{k|k-1}^g$ of the group center, the resolution matrix $\mathbf{A}_c$ describing the resolution cells in Cartesian coordinates proves to be time dependent and results from the matrix $\mathbf{A}$ by applying a rotation $\mathbf{D}_{\varphi_{k|k-1}^g}$ around $\varphi_{k|k-1}^g$ and a dilatation $\mathrm{diag}[1, r_{k|k-1}^g]$:

$$\mathbf{A}_c = \mathbf{D}_{\varphi_{k|k-1}^g} \begin{pmatrix} \alpha_r^2 & 0 \\ 0 & (r_{k|k-1}^g \alpha_\varphi)^2 \end{pmatrix} \mathbf{D}_{\varphi_{k|k-1}^g}^\top. \tag{55}$$

In the same way as the Cartesian measurement error ellipses, the Cartesian "resolution ellipses" depend on the target range. Suppose we have $\alpha_r = 100$ m and $\alpha_\varphi = 1°$, then we expect that the resolution in a distance of 50 km is about 100 m (range) and 900 m (cross range). As for military targets in a formation their mutual distance may well be 200 - 500 m or even less, resolution is a real target tracking problem[6].

3.3 Likelihood Functions

The likelihood functions proportional to the conditional probability density $p(Z_k, n_k | \mathbf{x}_k)$ statistically describe what a single frame of n_k observations $Z_k = \{\mathbf{z}_k^j\}_{j=1}^{n_k}$ can say about the single/joint state $\mathbf{x}_k$ of the objects to be tracked. Due to the Total Probability Theorem, $p(Z_k, n_k | \mathbf{x}_k)$ can be written as a sum over all possible data interpretations E_k, i.e. over all hypotheses regarding the origin of the data set Z_k:

$$p(Z_k, n_k | \mathbf{x}_k) = \sum_j p(Z_k, n_k, E_j | \mathbf{x}_k) \tag{56}$$

$$= \sum_j p(Z_k, n_k | E_j, \mathbf{x}_k) \, p(E_j | \mathbf{x}_k) \tag{57}$$

As shown below, the probability $P(E_j | \mathbf{x}_k)$ of E_j being correct as well as the individual likelihood functions $p(Z_k, n_k | E_j, x_k) = p(Z_k | E_j, n_k, \mathbf{x}_k) \, p(n_k | E_j)$ directly result from the statistical sensor model previously discussed (eqs. 45, 46, 47, 53). These considerations make evident that the determination of mutually exclusive and exhaustive data interpretations is prerequisite to sensor data processing. Though this is in general by no means a trivial task, in many practical cases a given multiple-object tracking problem can be decomposed into independent sub-problems of reduced complexity. We consider two examples that are practically important, but can still be handled more or less rigorously.

3.3.1 Well-separated Targets

For well-separated objects in a cluttered environment essentially two classes of data interpretations can be identified [3]:

1. E_0: The object considered was not detected, all n_k sensor returns in Z_k are false, i.e. assumed to be equally distributed in FoV (one interpretation).

2. $E_j, j = 1, \ldots, n_k$: The object was detected, $\mathbf{z}_k^j \in Z_k$ is the corresponding measurement, all other sensor returns are false (n_k interpretation hypotheses).

Standard probability reasoning yields:

$$p(E_j | \mathbf{x}_k) = \begin{cases} 1 - P_D & j = 0 \\ \frac{1}{n_k} P_D & j \neq 0 \end{cases} \tag{58}$$

$$p(Z_k, n_k | E_j, \mathbf{x}_k) = \begin{cases} p_F(n_k) \, |\text{FoV}|^{-n_k} & j = 0 \\ p_F(n_k - 1) \, |\text{FoV}|^{n_k - 1} \, \mathcal{N}(\mathbf{z}_k^j; \mathbf{H}\mathbf{x}_k, \mathbf{R}) & j \neq 0. \end{cases} \tag{59}$$

With $p_F(n_k)$ given by Equation 45, the conditional pdf $p(Z_k, n_k | \mathbf{x}_k)$ is proportional to the sum:

$$p(Z_k, n_k | \mathbf{x}_k) \propto (1 - P_D) \, \rho_F + P_D \sum_{j=1}^{n_k} \mathcal{N}(\mathbf{z}_k^j; \mathbf{H}_k \mathbf{x}_k, \mathbf{R}_k). \tag{60}$$

up to a factor $\frac{1}{n_k!} \, \rho_F^{n_k - 1} \, |\text{FoV}|^{-n_k} \, e^{-|\text{FoV}|\rho_F}$ being independent of the kinematical target state $\mathbf{x}_k$.

3.3.2 Target Formations

For a cluster of two closely-spaced objects moving in a cluttered environment five different classes of data interpretations exist ($\mathbf{x}_k = (\mathbf{x}_k^1, \mathbf{x}_k^2)^\top$) [20]:

1. E_{ii}, $i = 1, \ldots, n_k$: Both objects were not resolved but detected as a group, $\mathbf{z}_k^i \in Z_k$ represents the group measurement, all remaining returns are false (n_k data interpretations):

$$p(Z_k, n_k | E_{ii}, \mathbf{x}_k) = |\text{FoV}|^{1-n_k} \; \mathcal{N}(\mathbf{z}_k^i; \mathbf{H}_k^g \mathbf{x}_k, \mathbf{R}_k^g) \, p_F(n_k - 1) \tag{61}$$

$$P(E_{ii} | \mathbf{x}_k) = \frac{1}{n_k} \, P_u(\mathbf{x}_k) \, P_D^u. \tag{62}$$

With P_u as represented in Equation 53, $p(Z_k, n_k, E_k^{ii} | \mathbf{x}_k)$ is up to a constant factor given by:

$$p(Z_k, n_k, E_k^{ii} | \mathbf{x}_k) \propto \mathcal{N}\left(\begin{pmatrix} \mathbf{z}_k^i \\ 0 \end{pmatrix}; \begin{pmatrix} \mathbf{H}_g \\ \mathbf{H}_u \end{pmatrix} \mathbf{x}_k, \begin{pmatrix} \mathbf{R}_g & \mathbf{O} \\ \mathbf{O} & \mathbf{R}_u \end{pmatrix} \right). \tag{63}$$

Hence under the hypothesis E_k^{ii} two measurements are to be processed: the (real) plot $\mathbf{z}_k^i$ of the group center $\mathbf{H}_k^g \mathbf{x}_k = \frac{1}{2} \mathbf{H}(\mathbf{x}_k^1 + \mathbf{x}_k^2)$ and a (ficticious) measurement 'zero' of the distance $\mathbf{H}_u \mathbf{x}_k = \mathbf{H}(\mathbf{x}_k^1 - \mathbf{x}_k^2)$ between the objects. We can thus speak of *'negative' sensor information* [15], as the lack of a second target measurement conveys information on the target position. For in case of a resolution conflict the relative target distance must be smaller than the resolution.

2. E_0: Both objects were neither resolved nor detected as a group, all returns in Z_k are thus assumed to be false (one interpretation hypothesis):

$$p(Z_k, n_k | E_0, x_k) = P_u(\mathbf{x}_k) \, (1 - P_D^u) \, p_F(n_k) \tag{64}$$

$$P(E_0 | \mathbf{x}_k) = P_u(\mathbf{x}_k) \, (1 - P_D^u). \tag{65}$$

In analogy to the previous considerations we can write up to a constant factor:

$$p(Z_k, n_k, E_k^{00} | \mathbf{x}_k) \propto \mathcal{N}(0; \mathbf{H}_u \mathbf{x}, \mathbf{R}_u). \tag{66}$$

This means that even under the hypothesis of a missing unresolved plot at least a ficticious distance measurement 0 is being processed with a measurement error given by the sensor resolution.

3. E_{ij}, $i, j = 1, \ldots, n_k$, $i \neq j$: Both objects were resolved and detected, $\mathbf{z}_k^i, z_k^j \in Z_k$ are the measurements, $n_k - 2$ returns are false ($n_k(n_k - 1)$ interpretations):

$$p(Z_k, n_k | E_{ij}, \mathbf{x}_k) = |\text{FoV}|^{2-n_k} \; \mathcal{N}(\mathbf{z}_k^i; \mathbf{H}_k \mathbf{x}_k^1, \mathbf{R}_k) \; \mathcal{N}(\mathbf{z}_k^j; \mathbf{H}_k \mathbf{x}_k^2, \mathbf{R}_k) \, p_F(n_k - 2) \tag{67}$$

$$P(E_{ij} | \mathbf{x}_k) = \frac{1}{n_k(n_k-1)} \left(1 - P_u(\mathbf{x}_k) \right) P_D^2. \tag{68}$$

According to the factor $1 - P_u(\mathbf{x}_k) = 1 - |2\pi \mathbf{R}_u|^{\frac{1}{2}} \; \mathcal{N}(0; \mathbf{H}_u \mathbf{x}, \mathbf{R}_u)$ the likelihood function becomes a mixture, in which *negative* weighting factors can occur. Nevertheless the coefficients sum up to one; the density $p(\mathbf{x}_k | \mathcal{Z}^k)$ is thus well-defined. This reflects the fact that in case of a resolved group the targets must have a certain minimum distance between each other which is given by the sensor resolution. Otherwise they would not have been resolvable.

4. E_{i0}, E_{0i}, $i = 1, \ldots, n_k$: Both objects were resolved but only one object was detected, $\mathbf{z}_k^i \in Z_k$ is the measurement, $n_k - 1$ returns in Z_k are false ($2n_k$ interpretations):

$$p(Z_k | E_{i0}, \mathbf{x}_k) = |\text{FoV}|^{1-n_k} \; \mathcal{N}(\mathbf{z}_k^i; \mathbf{H}_k \mathbf{x}_k^1, \mathbf{R}_k) \, p_F(n_k - 1) \tag{69}$$

$$P(E_{i0} | \mathbf{x}_k) = \frac{1}{n_k} \left(1 - P_u(\mathbf{x}_k) \right) P_D \, (1 - P_D). \tag{70}$$

5. E_{00}: The objects were resolved but not detected, all n_k plots in Z_k are false (one interpretation):

$$p(Z_k, n_k | E_{00}, x_k) = |\text{FoV}|^{-n_k} \, p_F(n_k) \tag{71}$$

$$P(E_{00} | \mathbf{x}_k) = \left(1 - P_u(\mathbf{x}_k) \right) (1 - P_D)^2. \tag{72}$$

As there exist $(n_k + 1)^2 + 1$ interpretation hypotheses, the ambiguity for even small clusters of closely-spaced objects is much higher than in the case of well-separated objects ($n_k + 1$ each). We thus expect that only small groups can be handled more or less rigorously. For larger clusters (raids of military aircraft, for instance) a collective treatment [**?**] seems to be reasonable until the group splits off into smaller sub-clusters or individual objects. Up to a factor $\frac{1}{n_k!} \rho_F^{n_k-2} |FoV|^{-n_k} e^{-|FoV|\rho_F}$ independent of $\mathbf{x}_k$ (eq. 45), the likelihood function of the sensor data,

$$p(Z_k, n_k|x_k) = p(Z_k, n_k, E_0) + \sum_{i,j=0}^{n_k} p(Z_k, E_{ij}, n_k|x_k), \tag{73}$$

is proportional to a sum of GAUSSians and a constant:

$$p(Z_k, n_k|\mathbf{x}_k) \propto \rho_F^2(1-P_D)^2\big(1-P_u(\mathbf{x}_k)\big) + \rho_F(1-P_D^u)P_u(\mathbf{x}_k) + P_D^u\rho_F P_u(\mathbf{x}_k) \sum_{i=1}^{n_k} \mathcal{N}(\mathbf{z}_k^i; \mathbf{H}_k^g\mathbf{x}_k, \mathbf{R}_k^g)$$

$$+ \rho_F P_D(1-P_D)\big(1-P_u(\mathbf{x}_k)\big) \sum_{i=1}^{n_k} \big\{ \mathcal{N}(\mathbf{z}_k^i; \mathbf{H}_k\mathbf{x}_k^1, \mathbf{R}_k) + \mathcal{N}(\mathbf{z}_k^i; \mathbf{H}_k\mathbf{x}_k^2, \mathbf{R}_k)\big\}$$

$$+ P_D^2\big(1-P_u(\mathbf{x}_k)\big) \sum_{\substack{i,j=1\\i\neq j}}^{n_k} p_k^{ij}(\mathbf{x}_k)\, \mathcal{N}(\mathbf{z}_k^i; \mathbf{H}_k\mathbf{x}_k^1, \mathbf{R}_k)\, \mathcal{N}(\mathbf{z}_k^j; \mathbf{H}_k\mathbf{x}_k^2, \mathbf{R}_k). \tag{74}$$

3.4 MHT Update Equations

The tracking problems considered here are inherently ambiguous due to sensor data of uncertain origin. For the sake of simplicity we concentrate on the case of well-separated target. The formalism discussed below, however, can directly be applied to small target groups if the likelihood function in Equation 74 is used instead.

As in the examples previously discussed, let E_l denote a specific interpretation of the sensor data Z_l at scan time t_l taken out of a set of mutually exclusive and exhaustive interpretation hypotheses. Accordingly, the k-tuple $H_k = (E_k, \ldots, E_1)$, consisting of consecutive data interpretations E_l, $1 \le l \le k$, up to the time t_k, is a particular interpretation hypothesis regarding the origin of the accumulated sensor data $\mathcal{Z}^k = \{Z_k, n_k, Z_{k-1}, n_{k-1}, \ldots, Z_1, n_1\}$. H_k is thus called an *interpretation history*. For each H_k the related *pre-histories* $H_{k-n} = (E_{k-n}, \ldots, E_1)$ provide possible interpretations of sensor data $\mathcal{Z}^{k-n}$ accumulated up to scan $k - n$. With $H_n^k = (E_k, \ldots, E_{k-n+1})$, the *recent history*, any H_k can be decomposed in $H_k = (H_n^k, H_{k-n})$.

Obviously, the each density $p(\mathbf{x}_k|\mathcal{Z}^k)$ can be written as a sum over all possible interpretation histories:

$$p(\mathbf{x}_k|\mathcal{Z}^k) = \sum_{H_k} p(\mathbf{x}_k, H_k|\mathcal{Z}^k) = \sum_{H_k} p(\mathbf{x}_k|H_k, \mathcal{Z}^k)\, p(H_k|\mathcal{Z}^k). \tag{75}$$

$p(\mathbf{x}_k|\mathcal{Z}^k)$ is thus a *finite mixture density*, i.e. a weighted sum of *component densities* $p(\mathbf{x}_k|H_k, \mathcal{Z}^k)$ that assume a particular interpretation history H_k to be true (given the data $\mathcal{Z}^k$). The corresponding *mixing weights* $p(H_k|\mathcal{Z}^k)$ sum up to one.

3.4.1 MHT Prediction

Let the pdf $p(\mathbf{x}_{k-1}|\mathcal{Z}^{k-1})$ at time t_{k-1} be given by the following weighted sum of GAUSSians:

$$p(\mathbf{x}_{k-1}|\mathcal{Z}^{k-1}) = \sum_{H_{k-1}} p_{H_{k-1}}\, \mathcal{N}(\mathbf{x}_{k-1}; \mathbf{x}_{H_{k-1}}, \mathbf{P}_{H_{k-1}}). \tag{76}$$

According to the GAUSS-MARKOV-Model of the target dynamics previously introduced (subsection 2.2.1), the predicted pdf $p(\mathbf{x}_k|\mathcal{Z}^{k-1})$ of the target state at time t_k is given by:

$$p(\mathbf{x}_k|\mathcal{Z}^{k-1}) = \int d\mathbf{x}_{k-1} \ p(\mathbf{x}_k|\mathbf{x}_{k-1}) \ p(\mathbf{x}_{k-1}|\mathcal{Z}^{k-1}) \qquad \text{(MARKOV model)} \tag{77}$$

$$= \sum_{H_{k-1}} p_{H_{k-1}} \ \mathcal{N}(\mathbf{x}_k; \mathbf{F}\mathbf{x}_{H_{k-1}}, \ \mathbf{F}\mathbf{P}_{H_{k-1}}\mathbf{F}^\top + \mathbf{D}). \tag{78}$$

3.4.2 MHT Filtering

Very similar to the proceeding in the case of KALMAN filtering we obtain the filtering update equations by exploiting the product formula (Equation 7):

$$p(\mathbf{x}_k|\mathcal{Z}^k) = \frac{p(Z_k, n_k|\mathbf{x}_k) \ p(\mathbf{x}_k|\mathcal{Z}^{k-1})}{\int d\mathbf{x}_k \ p(Z_k, n_k|\mathbf{x}_k) \ p(\mathbf{x}_k|\mathcal{Z}^{k-1})} \qquad \text{(BAYES' rule)} \tag{79}$$

$$= \frac{\left((1 - P_D) \ \rho_F + P_D \sum_{j=1}^{n_k} \ \mathcal{N}(\mathbf{z}_k^j; \mathbf{H}\mathbf{x}_k, \mathbf{R})\right) p(\mathbf{x}_k|\mathcal{Z}^{k-1})}{\int d\mathbf{x}_k \left((1 - P_D) \ \rho_F + P_D \sum_{j=1}^{n_k} \ \mathcal{N}(\mathbf{z}_k^j; \mathbf{H}\mathbf{x}_k, \mathbf{R})\right) p(\mathbf{x}_k|\mathcal{Z}^{k-1})} \tag{80}$$

$$= \sum_{H_k} p_{H_k} \ \mathcal{N}(\mathbf{x}_k; \mathbf{x}_{H_k}, \mathbf{P}_{H_k}). \tag{81}$$

The expectation $\mathbf{x}_{H_k}$ and covariance matrix $\mathbf{P}_{H_k}$ result from the KALMAN filtering formulae (Equation 22), while the weighting factors are essentially characterized by the corresponding innovations $\boldsymbol{\nu}_{H_k}$, the innovation covariance matrix $\mathbf{S}_{H_k}$, and the statistical weight of the corresponding pre-history $p_{H_{k-1}}$:

$$p_{H_k} = \frac{p_{H_k}^*}{\sum_{H_k} p_{H_k}^*} \quad \text{with} \quad p_{H_k}^* = p_{H_{k-1}} \times \begin{cases} (1 - P_D) \ \rho_F & \text{for} \quad E_k = E_k^0 \\ P_D \ \mathcal{N}(\boldsymbol{\nu}_{H_k}; \mathbf{o}, \mathbf{S}_{H_k}) & \text{for} \quad E_k = E_k^j \end{cases}. \tag{82}$$

3.4.3 MHT Retrodiction

Retrodiction is an iteration scheme for calculating the probability densities $p(\mathbf{x}_l|\mathcal{Z}^k)$, $l < k$, that describe the *past* states $\mathbf{x}_l$ given all available sensor information $\mathcal{Z}^k$ accumulated up to a later scan time $t_k > t_l$, typically the *current* time. The iteration is initiated by the filtering result $p(\mathbf{x}_k|\mathcal{Z}^k)$ at time t_k and describes the impact of newly available sensor data on our knowledge of the past. In close analogy to the previous reasoning, an application of the Total Probability Theorem yields:

$$p(\mathbf{x}_l|\mathcal{Z}^k) = \sum_{H_k} p(\mathbf{x}_l, H_k|\mathcal{Z}_k) = \sum_{H_k} \underbrace{p(\mathbf{x}_l|H_k, \mathcal{Z}^k)}_{\text{no ambiguity}} \underbrace{p(H_k|\mathcal{Z}^k)}_{\text{filtering}} \tag{83}$$

The calculation of $p(\mathbf{x}_l|H_k, \mathcal{Z}^k)$, i.e. given a particular interpretation history H_k, is thus as in subsection 2.3.4, i.e. for $P_D = 1$, $\rho_F = 0$:

$$p(\mathbf{x}_l|H_k, \mathcal{Z}^k) = \mathcal{N}(\mathbf{x}_l; \mathbf{x}_{H_k}(l|k), \mathbf{P}_{H_k}(l|k)) \tag{84}$$

where the parameters of the GAUSSian are given by:

$$\mathbf{x}_{H_k}(l|k) = \mathbf{x}_{H_k}(l|l) + \mathbf{W}_{H_k}(l|k) \left(\mathbf{x}_{H_k}(l+1|k) - \mathbf{x}_{H_k}(l+1|l)\right) \tag{85}$$

$$\mathbf{P}_{H_k}(l|k) = \mathbf{P}_{H_k}(l|l) + \mathbf{W}_{H_k}(l|k) \left(\mathbf{P}_{H_k}(l+1|k) - \mathbf{P}_{H_k}(l+1|l)\right) \mathbf{W}_{H_k}(l|k)^\top \tag{86}$$

$$\text{gain matrix:} \quad \mathbf{W}_{H_k}(l|k) = \mathbf{P}_{H_k}(l|l)\mathbf{F}_{l+1|l}^\top \mathbf{P}_{H_k}(l+1|l)^{-1}. \tag{87}$$

A direct consequence of these considerations is the notion of a *retrodicted probability* [7]. Due to $H_k = (H_l^k, H_l)$ and the Total Probability Theorem, the probability of H_l being correct given the accumulated data up to time t_k can be calculated by summing up the weighting factors of all its descendants at time t_k:

$$p(H_l|\mathcal{Z}^k) = \sum_{H_n^k} p(H_n^k, H_l|\mathcal{Z}^k). \tag{88}$$

This result can also be obtained by considering the following approximation:

$$p(\mathbf{x}_l|H_k, \mathcal{Z}^k) = \mathcal{N}\big(\mathbf{x}_l; \mathbf{x}_{H_k}(l|k), \mathbf{P}_{H_k}(l|k)\big) \approx \mathcal{N}\big(\mathbf{x}_l; \mathbf{x}_{H_k}(l|l), \mathbf{P}_{H_k}(l|l)\big), \tag{89}$$

i.e. if the RTS-step is omitted. This means in particular: strong descendants can make weak ancestors stronger; weak descendants can weaken also strong ancestors; if all descendants are deleted, also the ancestors die.

3.5 Suboptimal Realizations

Due to the uncertain origin of the sensor data, naively applied sensor data processing according to the previous formalism leads to memory explosions: The number of components in the mixture densities $p(\mathbf{x}_k|\mathcal{Z}^k)$ exponentially grow at each step. Suboptimal approximation techniques are therefore inevitable for any practical realization. Fortunately, the densities resulting from prediction and filtering are characterized by a finite number of modes that may be large and fluctuating but does not explosively grow. This is the rationale for adaptive approximation methods that keep the number of mixture components under control without disturbing the density iteration too seriously. In other words, the densities can often be approximated by mixtures with (far) less components. Provided the relevant features of the densities are preserved, the resulting suboptimal algorithms are expected to be close to optimal BAYESian filtering.

3.5.1 Moment Matching

Moment matching is an important approximation method, by which a pdf $p(x)$ with expectation $\mathbb{E}_p[x] = \mathbf{x}$ and a covariance matrix $\mathbb{E}_p[(x - \bar{\mathbf{x}})(x - \bar{\mathbf{x}})^\top] = \mathbf{P}$ is approximated by $p(x) \approx \mathcal{N}(x; \mathbf{x}, \mathbf{P})$. In the present context moment matching is applied to mixture densities of the form $p(x) = \sum_H p_H \mathcal{N}(x; \mathbf{x}_H, \mathbf{P}_H)$, i.e. to normal mixtures. In this case $\mathbf{x}$ and $\mathbf{P}$ are given by:

$$\mathbf{x} = \sum_H p_H \mathbf{x}_H \tag{90}$$

$$\mathbf{P} = \sum_H p_H \big\{\mathbf{P}_H + \overbrace{(\mathbf{x}_H - \mathbf{x})(\mathbf{x}_H - \mathbf{x})^\top}^{\text{spread term}}\big\} \tag{91}$$

(a)   (b)
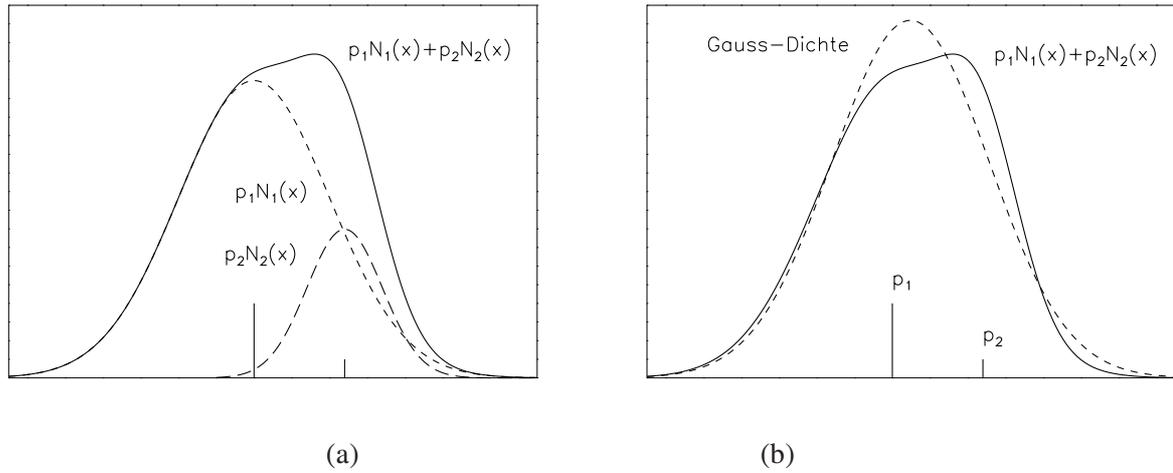
Figure 6: Scheme of Moment Matching

due to the following calculations:

$$\mathbb{E}_p[x] \;=\; \int dx\, x\, p(x) \;=\; \sum_H p_H \int dx\, x\, \mathcal{N}(x; \mathbf{x}_H, \mathbf{P}_H) \;=\; \sum_H p_H\, \mathbf{x}_H \;=:\; \mathbf{x}$$

$$\mathbb{C}_p[x] \;=\; \int dx\, p(x)\,(x - \mathbb{E}_p[x])(x - \mathbb{E}_p[x])^\top \;=\; \sum_H p_H \int dx\, (x-\mathbf{x})(x-\mathbf{x})^\top\, \mathcal{N}(x; \mathbf{x}_H, \mathbf{P}_H)$$

$$=\; \sum_H p_H \int dx\, \left\{ (x-\mathbf{x})(x-\mathbf{x})^\top - 2(x-\mathbf{x}_H)(\mathbf{x}_H - \mathbf{x})^\top \right\} \mathcal{N}(x; \mathbf{x}_H, \mathbf{P}_H)$$

$$\text{according to: } \int dx\, (x-\mathbf{x}_H)(\mathbf{x}_H - \mathbf{x})^\top\, \mathcal{N}(x; \mathbf{x}_H, \mathbf{P}_H) = 0$$

$$=\; \sum_H p_H \int dx\, \left\{ xx^\top - 2x\mathbf{x}_H^\top + \mathbf{x}_H\mathbf{x}_H^\top + \mathbf{x}_H\mathbf{x}_H^\top - 2\mathbf{x}_H\mathbf{x}^\top + \mathbf{x}\mathbf{x}^\top \right\} \mathcal{N}(x; \mathbf{x}_H, \mathbf{P}_H)$$

$$=\; \sum_H p_H \int dx\, \left\{ (x-\mathbf{x}_H)(x-\mathbf{x}_H)^\top + (\mathbf{x}_H - \mathbf{x})(\mathbf{x}_H - \mathbf{x})^\top \right\} \mathcal{N}(x; \mathbf{x}_H, \mathbf{P}_H)$$

$$=\; \sum_H p_H \left\{ \mathbf{P}_H + (\mathbf{x}_H - \mathbf{x})(\mathbf{x}_H - \mathbf{x})^\top \right\} \;=\; \mathbf{P}.$$

Figure 6 provides a schematic illustration of moment matching. A particular mixture density $p(x) = c_1 p_1(x) + c_2 p_2(x)$ is displayed along with the related mixture components $c_1 p_1(x)$, $c_1 p_1(x)$ (Figure 6a). In Figure 6b the mixture $p(x)$ is compared with the Gaussian density $\mathcal{N}(x; \mathbf{x}, \mathbf{P})$ with $\mathbf{x} = \mathbb{E}_p[x]$, $\mathbf{P} = \mathbb{E}_p[(x - \mathbf{x})^2]$. The bars at the bottom line indicate the relative size of the mixture coefficients c_1, c_2 in this example. Evidently, moment matching can provide a satisfying approximations to a mixture as long as it is unimodal.

3.5.2 Single Hypothesis

A radical solution to the growing memory problem is given by mono-hypothesis approximations briefly sketched below:

- Exclusion of competing sensor data by testing if $||v^i_{k|k-1}|| > \lambda$: "Gating". If this is successful we obtain KALMAN filtering as a limiting case.

(+) Gating is very simple (–) If λ is too small, the actual target measurement may be excluded.

- Forcing a unique interpretation in case of conflict. This means that the measurement with the minimum statistical distance from the expected measurement is used for updating: $\min_i ||\mathbf{v}_{k|k-1}^i||$. The resulting filter is called "Nearest-Neighbor-Filter (NN)".

  (+) One resultant hypothesis. (–) A hard decision is taken, which my be wrong. (–) NN is not adaptive.

- In case of "global combining" all hypotheses are merged to one single representative hypothesis. The resulting filter is called "(Joint) Probabilistic Data Association Filter (J)PADF".

  (+) All sensor data are used, (+) PDAF is adaptive. (–) Its applicability is limited.

Due to its importance, let us take a closer look at the PDAF filter. It is formally analog to the KALMAN filtering. The basic processing scheme is given by:

$$\textbf{filtering (scan } k-1\textbf{):} \quad p(\mathbf{x}_{k-1}|\mathcal{Z}^{k-1}) \;=\; \mathcal{N}(\mathbf{x}_{k-1};\, \mathbf{x}_{k-1|k-1}, \mathbf{P}_{k-1|k-1}) \;(\rightarrow \text{initiation})$$

$$\textbf{prediction (scan } k\textbf{):} \quad p(\mathbf{x}_k|\mathcal{Z}^{k-1}) \;\approx\; \mathcal{N}(\mathbf{x}_k;\, \mathbf{x}_{k|k-1}, \mathbf{P}_{k|k-1}) \;\text{ (as usual)}$$

$$\textbf{filtering (scan } k\textbf{):} \quad p(\mathbf{x}_k|\mathcal{Z}^k) \;\approx\; \sum_{j=0}^{n_k} p_k^j\, \mathcal{N}(\mathbf{x}_k;\, \mathbf{x}_{k|k}^j, \mathbf{P}_{k|k}^j) \;\approx\; \mathcal{N}(\mathbf{x}_k;\, \mathbf{x}_{k|k}, \mathbf{P}_{k|k})$$

where the quantities $\mathbf{x}_{k|k}^j,\, \mathbf{P}_{k|k}^j,\, p_k^j$ are to be calculated as follows:

$$\mathbf{x}_{k|k}^j = \begin{cases} \mathbf{x}_{k|k-1} & j=0 \\ \mathbf{x}_{k|k-1} + \mathbf{W}_k \mathbf{v}_k^j & j\neq 0 \end{cases} \qquad \mathbf{P}_{k|k}^j = \begin{cases} \mathbf{P}_{k|k-1} & j=0 \\ \mathbf{P}_{k|k-1} - \mathbf{W}_k \mathbf{S}_k \mathbf{W}_k^\top & j\neq 0 \end{cases}$$

$$\text{with:} \quad \mathbf{v}_k^j = \underbrace{\mathbf{z}_k^j - \mathbf{H}\mathbf{x}_k}_{\text{innovation}}, \qquad \mathbf{W}_k = \underbrace{\mathbf{P}_{k|k-1}\mathbf{H}^\top \mathbf{S}_k^{-1}}_{\text{gain matrix}}, \qquad \mathbf{S}_k = \underbrace{\mathbf{H}\mathbf{P}_{k|k-1}\mathbf{H}^\top + \mathbf{R}}_{\text{innovation covariance}}$$

$$p_k^j = \underbrace{\frac{p_k^{j*}}{\sum_j p_k^{j*}}}_{\text{weights}}, \qquad p_k^{j*} = \begin{cases} (1-P_D)\,\rho_F & j=0 \\ P_D\, \mathcal{N}(\mathbf{v}_k^j, \mathbf{S}_k) & j\neq 0 \end{cases}.$$

With the *combined innovation* $\mathbf{v}_k = \sum_{j=0}^{n_k} p_k^j \mathbf{v}_k^j$ we obtain by moment matching:

$$\mathbf{x}_{k|k} = \sum_{j=0}^{n_k} p_k^j \mathbf{x}_{k|k}^j = p_k^0 \mathbf{x}_{k|k-1} + \sum_{j=1}^{n_k} p_k^j \big(\mathbf{x}_{k|k-1} + \mathbf{W}_k \mathbf{v}_k^j\big) = \mathbf{x}_{k|k-1} + \mathbf{W}_k\, \mathbf{v}_k \tag{92}$$

$$\mathbf{P}_{k|k} = \sum_{j=0}^{n_k} p_k^j \big(\mathbf{P}_{k|k}^j + (\mathbf{x}_{k|k}^j - \mathbf{x}_{k|k})(\mathbf{x}_{k|k}^j - \mathbf{x}_{k|k})^\top\big) \tag{93}$$

$$= \mathbf{P}_{k|k-1} - \sum_{j=1}^{n_k} p_k^j \mathbf{W}_k \mathbf{S}_k \mathbf{W}_k^\top + \sum_{j=1}^{n_k} p_k^j \mathbf{W}_k (\mathbf{v}_k^j - \mathbf{v}_k)(\mathbf{v}_k^j - \mathbf{v}_k)^\top \mathbf{W}_k^\top \tag{94}$$

$$= \mathbf{P}_{k|k-1} - (1-p_k^0)\mathbf{W}_k \mathbf{S}_k \mathbf{W}_k^\top + \mathbf{W}_k \Big[\underbrace{\sum_{j=1}^{n_k} p_k^j \mathbf{v}_k^j \mathbf{v}_k^{j\top} - \mathbf{v}_k \mathbf{v}_k^\top}_{\text{spread of innovations}} \Big] \mathbf{W}_k^\top. \tag{95}$$

3.5.3 Multiple Hypotheses

In case of a more severe false return background or in a multiple-object tracking task with correlation gates overlapping for a longer time, Bayesian track maintenance inevitably leads to densities $p(\mathbf{x}_k|\mathcal{Z}^k)$ that are characterized by several distinct modes. As this phenomenon is inherent in the uncertain origin of the received data, relevant statistical information would get lost if global combining is applied to such cases. The use of PDA-type filtering is thus confined to a relatively restricted area in parameter space (defined by ρ_F, P_D, for instance).

By *local* combining of suitably chosen sub-mixtures and pruning of irrelevant mixture components, however, memory explosions may be avoided without destroying the multi-mode structure of the densities. Provided this is carefully done with data-driven adaptivity, all statistically relevant information may be preserved while keeping the number of mixture components under control, i.e. the number may be fluctuating and be even large in critical situations but does not explosively grow. Evidently, PDA-type filtering is a limiting case of such MHT-type techniques.

Individual Gating. In a first step for avoiding unnecessary computational load, sensor data irrelevant for a given track hypothesis are excluded. Individual gating means that only those sensor data are used for continuing a particular track hypothesis H_k whose innovations obey: $\boldsymbol{\nu}_{H_k}^\top \mathbf{S}_{H_k}^{-1} \boldsymbol{\nu}_{H_k} < \lambda$. The processing parameter λ must be tuned to meet the requirements of a particular application. Evidently, the accuracy of the prediction (depending on the system dynamics model and the previous track hypothesis) and a priori information on the sensor performance enters into this decision criterion. Individual gating is a simple measure of pre-selecting the sensor data. It can be performed for each track hypothesis independently before any further data processing takes place.

Pruning Methods. In order to identify insignificant track hypotheses, first for each H^k the weighting factors p_{H_k} are evaluated by processing the sensor data within the gates. This is done before the hypothetical tracks $\mathbf{x}_{H_k}$, $\mathbf{P}_{H_k}$ are computed. Due to the normalization involved, the size of each weighting factor p_{H_k} depends on all sensor data in the gates. In contrast to individual gating, pruning is therefore applied after all weighting factors are available. In *zero-scan pruning* track hypotheses are deleted that are smaller than a certain predefined threshold. By this, an additional processing parameter is introduced that must be tuned to meet the requirements of a particular application. The limiting case where the track hypothesis of highest statistical weight is considered only, is a slightly more general formulation of standard Nearest-Neighbor filtering as the hypothesis of a missing measurement may be of highest weight. *Delayed* or *multiple-frame pruning* is closely related to this procedure. Here we consider the retrodicted weighting factors for a past time given all sensor data up to the current scan (see subsection 3.4.3).

Local Combining. After filtering a single distinct mode of $p(\mathbf{x}_k|\mathcal{Z}^k)$ might be a superposition of "similar" mixture components. It is thus reasonable to apply local combining to the sub-mixture producing that mode. Among several realizations *successive local combining* is particularly simple. Let us start with the mixture component of highest statistical weight. In the order of decreasing weighting factors a component is searched that is "similar" to the previous one. A very simple scalar criterion for similarity is provided by:

$$d(H_k^1, H_k^2) < \kappa \quad \text{with:} \quad d(H_k^1, H_k^2) = (\mathbf{x}_{H_k^1} - \mathbf{x}_{H_k^2})^\top (\mathbf{P}_{H_k^1} + \mathbf{P}_{H_k^2})^{-1}(\mathbf{x}_{H_k^1} - \mathbf{x}_{H_k^2}), \tag{96}$$

where $\mathbf{x}_{H_k^{1,2}}$ and $\mathbf{P}_{H_k^{1,2}}$ denote the mean and covariance of the components. By this, a third processing parameter κ is introduced (besides λ and the pruning parameter) that must be tuned to meet the requirements of a particular application. Local combining results in an 'effective' component with an increased weighting factor. Then the next similar component is searched in the order of decreasing weighting factors and so on. Having done this, we restart the procedure with the mixture component having the second largest weighting

factor. Due to the data-driven adaptivity inherent in this method, MHT-type filtering automatically reduces to PDA-type processing if PDA-processing provides good approximations to $p(\mathbf{x}_k|\mathcal{Z}^k)$.

Objects moving closely-spaced for some time may irreversibly loose their identity: When they dissolve again, a unique track-to-target association is impossible. In particular, this means that the component densities $p(\mathbf{x}_k, H_k^1|\mathcal{Z}^k)$ and $p(\mathbf{x}_k, H_k^2|\mathcal{Z}^k)$ are nearly identical if H_k^1 and H_k^2 differ only in a permutation of the targets. It is thus reasonable to deal with densities that are symmetric under permutations of the individual targets. By this, no statistically relevant information is lost and the filter performance remains unchanged, while the mean number of hypotheses involved may be significantly reduced.

3.6 Sequential Track Extraction

After solving the 'track maintenance' problem by deriving iterative processing schemes for updating conditional probability densities, an important question is still open: By which means can the iteration process be started? This is by no means a trivial task in case of ambiguous sensor data.

The initiation of the pdf-iteration is based on 'extracted' target tracks, i.e. on tracks whose existence is 'detected' by a detection process on a higher level of abstraction, which makes use of sensor detections accumulated over time. More strictly speaking, we have to find a candidate for a target track in a time series of sensor observations $\mathcal{Z}^k = \{Z_i\}_{i=1}^k$. For the sake of simplicity we assume for the time being: 1. In the FoV of the sensors there is at most one object. 2. The sensor data collected in one scan are measured at the same time.

We have to decide between two hypotheses:

- h_1: Besides false returns, $\mathcal{Z}^k$ contains also actual target measurements.

- h_0: There is no target existing in the FoV; all sensor data in $\mathcal{Z}^k$ are false.

Two decision errors are involved characterizing the performance of any test procedure: 1. The conditional probability that hypothesis h_1 is accepted given h_1 is actually true $P_1 = \text{Prob}(accept\ h_1|h_1)$ corresponding to the detection probability P_D of a sensor. 2. $P_0 = \text{Prob}(accept\ h_1|h_0)$, corresponding to the false alarm probability P_F.

3.6.1 Likelihood-ratio Test

We are looking for a test procedure for deciding between these two probabilities as quickly as possible for given decision errors P_0, P_1. Let us consider the conditional probability densities $p(\mathcal{Z}^k|h_0)$, $p(\mathcal{Z}^k|h_1)$ (likelihood functions) and an intuitively plausible test function (likelihood ratio):

$$\text{LR}(k) = \frac{p(\mathcal{Z}^k|h_1)}{p(\mathcal{Z}^k|h_0)}. \tag{97}$$

Starting from a time window of length $k = 1$, the test function $\text{LR}(k)$ is successively calculated and compared with two thresholds A and B:

	for	$\text{LR}(k) < A$,	accept the hypothesis h_0 (i.e. no object existent in the FoV)
	for	$\text{LR}(k) > B$,	accept the hypothesis h_1 (i.e. an object exists in the FoV)
	for	$A < \text{LR}(k) < B$,	expect new data Z_{k+1} and repeat the test with $\text{LR}(k+1)$.

This test procedure (*sequential likelihood ratio test*) has the following, practically important properties:

1. For the detection thresholds A, B and the decision errors P_0, P_1 obey approximately the relationship:

$$A \approx \frac{1 - P_1}{1 - P_0} \quad \text{and} \quad B \approx \frac{P_1}{P_0}. \tag{98}$$

2. The actual decision time required, i.e. the amount of sensor data required, is a random quantity.

3. On average the sequential likelihood test has a *minimal* decision length for given errors P_0, P_1.

4. The actual choice of P_0 (P_1) has impact on the *mean* decision length assuming h_1 (h_0) is valid.

5. In practice the parameter P_1 is chosen close to One for actually detecting real object tracks.

6. The parameter P_0 should be small, as the tracking system is not to be overloaded with false tracks.

3.6.2 Iterative Updating

For calculating the likelihood ratio, interpretations histories $H_k = \{E_k, H_{k-1}\}$ of the accumulated data $\mathcal{Z}^k = \{Z_k, \mathcal{Z}^{k-1}\}$ have to be considered as before in the case of track maintenance. With $E_k = E_k^0$ (Object not detected), $E_k = E_k^j$ ($\mathbf{z}_k^j \in Z_k$ is the target measurement) and with the histories H_k we can write:

$$\text{LR}(k) = \frac{p(\mathcal{Z}^k | h_1)}{p(\mathcal{Z}^k | h_0)} = \frac{\sum_{H_k} p(\mathcal{Z}^k, H_k | h_1)}{p(\mathcal{Z}^k | h_0)} = \frac{\sum_{H_k} p(\mathcal{Z}^k | H_k, h_1)\, p(H_k | h_1)}{p(\mathcal{Z}^k | h_0)}. \tag{99}$$

For the test procedure an *iterative* calculation is requested. Standard probability reasoning yields:

$$p(H_k | h_1) = p(E_k | H_{k-1}, h_1)\, p(H_{k-1} | h_1) = p(H_{k-1} | h_1) \begin{cases} (1 - P_D)\, p_F(n_k) & E_k = E_k^0 \\ \frac{P_d}{n_k}\, p_F(n_k - 1) & E_k = E_k^j \end{cases} \tag{100}$$

$$p(\mathcal{Z}^k | H_k, h_1) = p(Z_k | H_k, \mathcal{Z}^{k-1}, h_1)\, p(\mathcal{Z}^{k-1} | H_{k-1}, h_1) \tag{101}$$

$$= p(\mathcal{Z}^{k-1} | H_{k-1}, h_1) \begin{cases} |\text{FoV}|^{-n_k} & E_k = E_k^0 \\ |\text{FoV}|^{-n_k+1}\, \mathcal{N}(\boldsymbol{v}_{H_k}, \mathbf{S}_{H_k}) & E_k = E_k^j \end{cases} \tag{102}$$

$$p(\mathcal{Z}^k | h_0) = p(Z_k, n_k, \mathcal{Z}^{k-1} | h_0) = p(Z_k | n_k, \mathcal{Z}^{k-1}, h_0)\, p(n_k | \mathcal{Z}^{k-1}, h_0)\, p(\mathcal{Z}^{k-1} | h_0) \tag{103}$$

$$= |\text{FoV}|^{-n_k}\, p_F(n_k)\, p(\mathcal{Z}^{k-1} | h_0) \qquad \text{with:} \qquad p_F(n_k) = \frac{\rho_F |\text{FoV}|}{n_k!}\, \mathrm{e}^{-\rho_F |\text{FoV}|}. \tag{104}$$

We consider the following, convenient notation for multiple sums:

$$\mathbf{j}_k = (j_k, \ldots, j_1) \quad \text{let us write} \quad \sum_{\mathbf{j}_k} \lambda_{\mathbf{j}_k} = \sum_{j_k=0}^{n_k} \cdots \sum_{j_1=0}^{n_1} \lambda_{j_k \ldots j_1}. \tag{105}$$

From the formulae above an application of the product formulae (Equation 7) results in the following simple update formulae for the likelihood ratio:

$$\textbf{Initiation:} \qquad k = 0, \quad \mathbf{j}_0 = 0, \quad \lambda_{\mathbf{j}_0} = 1 \tag{106}$$

$$\textbf{Updating:} \qquad \text{LR}(k + 1) = \sum_{\mathbf{j}_{k+1}} \lambda_{\mathbf{j}_{k+1}} = \sum_{j_{k+1}=0}^{n_{k+1}} \sum_{\mathbf{j}_k} \lambda_{j_{k+1}\mathbf{j}_k}\, \lambda_{\mathbf{j}_k} \tag{107}$$

$$\text{with:} \qquad \lambda_{j_{k+1}\mathbf{j}_k} = \begin{cases} 1 - P_D & \text{for:} \quad j_{k+1} = 0 \\ \frac{P_D}{\rho_F}\, \mathcal{N}(\boldsymbol{v}_{j_{k+1}\mathbf{j}_k}, \mathbf{S}_{j_{k+1}\mathbf{j}_k}) & \text{for:} \quad j_{k+1} \neq 0 \end{cases} \tag{108}$$

$$\text{senor data innovation:} \qquad \boldsymbol{\nu}_{j_{k+1}\mathbf{j}_k} = \mathbf{z}_{j_{k+1}} - \mathbf{H}_{j_{k+1}}\mathbf{x}_{\mathbf{j}_{k+1|k}} \qquad (109)$$

$$\text{innovation covariance:} \qquad \mathbf{S}_{j_{k+1}\mathbf{j}_k} = \mathbf{H}_{j_{k+1}}\mathbf{P}_{\mathbf{j}_{k+1|k}}\mathbf{H}_{j_{k+1}}^\top + \mathbf{R}_{j_{k+1}} \qquad (110)$$

$$\text{state update:} \qquad \mathbf{x}_{\mathbf{j}_{k+1|k}} = \mathbf{F}_{j_{k+1}}\mathbf{x}_{\mathbf{j}_k} \qquad\qquad \mathbf{x}_{\mathbf{j}_k} = \mathbf{x}_{\mathbf{j}_{k|k-1}} + \mathbf{W}_{j_k\mathbf{j}_{k-1}}\boldsymbol{\nu}_{j_k,\mathbf{j}_{k-1}} \qquad (111)$$

$$\text{covariances:} \qquad \mathbf{P}_{\mathbf{j}_{k+1|k}} = \mathbf{F}_{j_{k+1}}\mathbf{P}_{\mathbf{j}_k}\mathbf{F}_{j_{k+1}}^\top + \mathbf{D}_{j_{k+1}} \quad \mathbf{P}_{\mathbf{j}_k} = \mathbf{P}_{\mathbf{j}_{k|k-1}} - \mathbf{W}_{j_k\mathbf{j}_{k-1}}\mathbf{S}_{j_k\mathbf{j}_{k-1}}\mathbf{W}_{j_k\mathbf{j}_{k-1}}^\top \qquad (112)$$

$$\text{KALMAN gain:} \qquad \mathbf{W}_{j_k\mathbf{j}_{k-1}} = \mathbf{P}_{\mathbf{j}_{k|k-1}}\mathbf{H}_{j_k}^\top \mathbf{S}_{j_k\mathbf{j}_{k-1}}^{-1}. \qquad (113)$$

3.6.3 Hand-over to Maintenance

The further proceeding in sequential track extraction consists of the following steps:

- $\text{LR}(k)$ is represented by an increasing number of summands, which are related to a particular interpretation history. The tuple $\{\lambda_{\mathbf{j}_k}, \mathbf{x}_{\mathbf{j}_k} \mathbf{P}_{\mathbf{j}_k}\}$ is called a *sub-track*.

- For mitigating the growing-memory problem all approximations are to be used which have been introduced for MHT track maintenance, as far as they do no significantly affect $\text{LR}(k)$:

  - *Individual gating:* Exclude data whose association to an existing sub-track is too improbable.
  - *Pruning:* Delete sub-tacks which contribute not significantly to the likelihood ratio.
  - *Local combining:* Merge *similar* sub-tracks by using moment matching according to

$$\{\lambda_i, \mathbf{x}_i, \mathbf{P}_i\}_i \ \rightarrow\ \{\lambda, \mathbf{x}, \mathbf{P}\} \quad \text{with:} \quad \lambda = \sum_i \lambda_i \qquad (114)$$

$$\mathbf{x} = \frac{1}{\lambda}\sum_i \lambda_i \mathbf{x}_i, \quad \mathbf{P} = \frac{1}{\lambda}\sum_i \lambda_i[\mathbf{P}_i + (\mathbf{x}_i - \mathbf{x})(\ldots)^\top]. \qquad (115)$$

- The test ends with a decision in favor of one of the hypotheses: h_0 (no object) or h_1 (object existent).

- After a track detection, the pdf for track maintenance is initiated by the sub-tracks according to:

$$\text{normalization of the coefficients } \lambda_{\mathbf{j}_k}: \qquad p_{\mathbf{j}_k} = \frac{\lambda_{\mathbf{j}_k}}{\sum_{\mathbf{j}_k} \lambda_{\mathbf{j}_k}} \qquad (116)$$

$$\{\lambda_{\mathbf{j}_k}, \mathbf{x}_{\mathbf{j}_k}, \mathbf{P}_{\mathbf{j}_k}\} \quad \rightarrow \quad p(\mathbf{x}_k|\mathcal{Z}^k) = \sum_{\mathbf{j}_k} p_{\mathbf{j}_k}\ \mathcal{N}(\mathbf{x}_k; \mathbf{x}_{\mathbf{j}_k}, \mathbf{P}_{\mathbf{j}_k}). \qquad (117)$$

- After a successful track extraction the sequential likelihood ratio test is restarted and exploits the remaining sensor data not used for maintaining the existent tracks. Eventually other tracks can be extracted.

- The sequential likelihood ration test can be used for *track censoring*: After a decision in favor of h_1 we set: $\text{LR}(0) = 1$ and calculate $\text{LR}(k)$ from the parameters defining $p(\mathbf{x}_k|\mathcal{Z}^k)$:

  - *Track confirmation:* $\quad \text{LR}(k) > \frac{P_1}{P_0}, \quad$ re-start: $\text{LR}(0) = 1$.
  - *Track Deletion:* $\quad \text{LR}(k) < \frac{1-P_1}{1-P_0}, \quad$ (eventually re-extraction of the target)

3.6.4   Extension: Target Cluster

The previously discussed track extraction scheme can directly be generalized to target clusters if the number n of objects within the cluster is known. For the sake of simplicity we let us assume an ideal resolution capability of the sensor. In the case of an *unknown* number of objects we can proceed as follows:

1. Start the track extraction for the target cluster with the scan Z_1 of sensor measurements.

2. Assume a maximum number N of objects within the target cluster, i.e. we have $n < N$.

3. Let the a priori probability of having n targets within the cluster be given by: $P(n) = \frac{1}{N}$.

4. Consider hypotheses h_n assuming n individual objects within the cluster (h_0: no object).

5. Assume that in the initial sensor data set Z_1 at least one object measurement is existent.

6. The generalized likelihood ratio test function is given by: $\mathrm{LR}(k) = \frac{1}{N} \sum_{n=1}^{N} \frac{p(\mathcal{Z}^k|h_n)}{p(\mathcal{Z}^k|h_0)}$.

7. The conditional likelihoods $p(\mathcal{Z}^k|h_n)$ and $p(\mathcal{Z}^k|h_0)$ are iteratively calculated as before.

3.7   Discussion of Examples

From our experiments with real radar data we learned the following lessons (for details see [21, 18]):

1. IMM-MHT is applicable in situations that are inaccessible to human radar operators.

2. The filter is rather robust and does not critically depend on modeling parameters (within certain limits).

3. Decisive are both, its *multiple hypothesis* character allowing tentative alternatives in critical situations and the *qualitatively correct modeling* of all significant effects.

4. Unless properly handled, resolution conflicts can seriously destabilize tracking.

5. Mono-hypothesis approximations to MHT (such as JPDAF) are not applicable in scenarios as considered in Figure 3.

6. MHT is highly adaptive, developing its multiple hypothesis character only when needed.

7. Retrodiction provides unique and accurate results from ambiguous MHT output if a small time delay is accepted (some frames).

8. The maximum gain achievable by retrodiction is roughly the same for both, worst-case modeling and IMM-MHT.

9. Algorithms employing multiple dynamics models are superior in that the time delays involved are shorter.

10. Finally, it seems notable that a very simplified modeling of the sensor, the target dynamics, and the environment may provide reasonable results if applied to real data.

References

[1] BALTES, R., KEUK, G.VAN, 'Tracking Multiple Maneuvering Targets in a Network of Passive Radars', IEEE International Radar Conference, Washington DC, 1995.

[2] BALTES, R., 'A Triangulation System for Tracking Multiple Targets with Passive Sensors', International Radar Symposium IRS'98, Muenchen, 1998.

[3] BAR-SHALOM, Y., LI, X.-R., AND KIRUBARAJAN, T., *Estimation with Applications to Tracking and Navigation*, Wiley & Sons, 2001.

[4] BLACKMAN, S., POPULI, R., *Design and Analysis of Modern Tracking Systems*, Artech House, 1999.

[5] BOGLER, PH.L., *Radar Principles with Applications to Tracking Systems*, John Wiley & Sons (1990).

[6] DAUM, F.E., FITZGERALD, R.J., 'The Importance of Resolution in Multiple Target Tracking', *SPIE 2235, Signal and Data Processing of Small Targets*, 329 (1994).q

[7] DRUMMOND, O.E., 'Target Tracking with Retrodicted Discrete Probabilities', *SPIE 3163, Signal and Data Processing of Small Targets*, 249 (1997).

[8] DRUMMOND, O.E. (ED.), 'Introduction', *SPIE 3373, Signal and Data Processing of Small Targets 1998*.

[9] GELB, A. (ED.), *Applied Optimal Estimation*, MIT Press (1974).

[10] HARVILLE, D. A., *Matrix Algebra from a Statistician's Perspective*, Springer (1997).

[11] KEUK, G.VAN, 'MHT Extraction and Track Maintenance of a Target Formation', *IEEE Transactions on Aerospace and Electronic Systems*, **38**, 288 (2002).

[12] VAN KEUK, 'Sequential Track Extraction', *IEEE Transactions on Aerospace and Electronic Systems*, **34**, 1135 (1998).

[13] VAN KEUK, G., 'Multihypothesis Tracking Using Incoherent Signal-Strength Information', *IEEE AES* **32**, No. 3 (1996).

[14] VAN KEUK, G., BLACKMAN, S.S., 'On Phased Array Radar Tracking and Parameter Control', *IEEE Transactions on Aerospace and Electronic Systems*, **29**, 186 (1993).

[15] KOCH, W., 'On Negative Information in Sensor Data Fusion: Discussion of Selected Examples'. In: *The 7th International Conference on Information Fusion*, June 2004, Stockholm, Sweden (to appear also in: *The Information Fusion Journal*, Elsevier, 2004).

[16] KOCH, W., Target Tracking. In: *Advanced Signal Processing Handbook: Theory and Applications for Radar, Sonar, and Medical Imaging Systems*, CRC Press, 2001.

[17] KOCH, W., 'Fixed-Interval Retrodiction Approach to Bayesian IMM-MHT for Maneuvering Multiple Targets', *IEEE Transactions on Aerospace and Electronic Systems*, **36**, No. 1, (2000).

[18] KOCH, W., 'Generalized Smoothing for Multiple Model/Multiple Hypothesis Filtering: Experimental Results', *ECC 99, European Control Conference*, 31.8.-3.9.1999, Karlsruhe, Germany.

[19] KOCH, W., 'On Adaptive Parameter Control for IMM-MHT Phased-Array Tracking', *SPIE 3809, Signal and Data Processing of Small Targets* (1999).

[20] KOCH, W., VAN KEUK, G., 'Multiple Hypothesis Track Maintenance with Possibly Unresolved Measurements', *IEEE AES 33*, No. 3 (1997).

[21] KOCH, W., 'Experimental Results on Bayesian MHT for Maneuvering Closely-Spaced Objects in a Densely Cluttered Environment', *RADAR 97, IEE International Radar Conference*, 729 (1997).

[22] KOCH, W., 'Retrodiction for Bayesian Multiple Hypothesis/Multiple Target Tracking in Densely Cluttered Environment', *SPIE 2759, Signal and Data Processing of Small Targets*, 429 (1996).

[23] RISTIC, B., GORDON, N., *Beyond Kalman Filtering*. Wiley, 2004.